

# ***MYCN* is amplified during S phase, and *c-myb* is involved in controlling *MYCN* expression and amplification in *MYCN*-amplified neuroblastoma cell lines**

NEVIM AYGUN and OGUZ ALTUNGOZ

Department of Medical Biology, Faculty of Medicine, Dokuz Eylul University, Izmir 35340, Turkey

Received December 20, 2017; Accepted October 3, 2018

DOI: 10.3892/mmr.2018.9686

**Abstract.** Neuroblastoma derived from primitive sympathetic neural precursors is a common type of solid tumor in infants. *MYCN* proto-oncogene bHLH transcription factor (*MYCN*) amplification and 1p36 deletion are important factors associated with the poor prognosis of neuroblastoma. Expression levels of *MYCN* and *c-MYB* proto-oncogene transcription factor (*c-myb*) decline during the differentiation of neuroblastoma cells; E2F transcription factor 1 (E2F1) activates the *MYCN* promoter. However, the underlying mechanism of *MYCN* overexpression and amplification requires further investigation. In the present study, potential *c-Myb* target genes, and the effect of *c-myb* RNA interference (RNAi) on *MYCN* expression and amplification were investigated in *MYCN*-amplified neuroblastoma cell lines. The mRNA expression levels and *MYCN* gene copy number in five neuroblastoma cell lines were determined by quantitative polymerase chain reaction. In addition, variations in potential target gene expression and *MYCN* gene copy number between pre- and post-*c-myb* RNAi treatment groups in *MYCN*-amplified Kelly, IMR32, SIMA and MHH-NB-11 cell lines, normalized to those of non-*MYCN*-amplified SH-SY5Y, were examined. To determine the associations between gene expression levels and chromosomal aberrations, *MYCN* amplification and 1p36 alterations in interphases/metaphases were analyzed using fluorescence *in situ* hybridization. Statistical analyses revealed correlations between 1p36 alterations and the expression of *c-myb*, *MYB* proto-oncogene like 2 (*B-myb*) and cyclin dependent kinase inhibitor 1A (*p21*).

Additionally, the results of the present study also demonstrated that *c-myb* may be associated with *E2F1* and *L3MBTL1* histone methyl-lysine binding protein (*L3MBTL1*) expression, and that *E2F1* may contribute to *MYCN*, *B-myb*, *p21* and chromatin licensing and DNA replication factor 1 (*hCdt1*) expression, but to the repression of *geminin* (*GMNN*). On *c-myb* RNAi treatment, *L3MBTL1* expression was silenced, while *GMNN* was upregulated, indicating G<sub>2</sub>/M arrest. In addition, *MYCN* gene copy number increased following treatment with *c-myb* RNAi. Notably, the present study also reported a 43.545% sequence identity between upstream of *MYCN* and *Drosophila melanogaster* amplification control element 3, suggesting that expression and/or amplification mechanisms of developmentally-regulated genes may be evolutionarily conserved. In conclusion, *c-myb* may be associated with regulating *MYCN* expression and amplification. *c-myb*, *B-myb* and *p21* may also serve a role against chromosome 1p aberrations. Together, it was concluded that *MYCN* gene is amplified during S phase, potentially via a replication-based mechanism.

## **Introduction**

*MYCN* proto-oncogene bHLH transcription factor (*MYCN*) amplification and 1p36 deletion are important factors associated with poor prognosis in neuroblastoma (1-3), one of the most types of infant malignancy (4). *MYCN* amplification, which leads to *MYCN* overexpression, has been reported in 18-38% of cases of neuroblastoma and in a panel of neuroblastoma cell lines (3,5-9). As a developmentally-regulated gene, *MYCN* is highly expressed in dorsal root ganglia, sympathetic chain ganglia and the spinal cord in the human fetus during the development of the sympathetic nervous system at 8.5 weeks of gestation (9). In addition, the chromosome 1p36 locus is frequently deleted in neuroblastoma cell lines (10). Chromodomain helicase DNA binding protein 5, calmodulin binding transcription activator 1, kinesin family member 1B  $\beta$ , castor zinc finger 1 and microRNA (miR)-34a have been analyzed as the strongest candidate tumor suppressor genes at the 1p36 locus in neuroblastoma (11,12).

*c-MYB* proto-oncogene transcription factor (*c-Myb*) has been reported to be associated with cell growth and proliferation in neuroblastoma (13). On induction by retinoic

---

**Correspondence to:** Dr Nevim Aygun, Department of Medical Biology, Faculty of Medicine, Dokuz Eylul University, Mithatpasa Street, Inciralti, Izmir 35340, Turkey  
E-mail: nevim.aygun@gmail.com

**Key words:** neuroblastoma, *MYCN* proto-oncogene bHLH transcription factor amplification, 1p36 deletion, *c-MYB* proto-oncogene transcription factor, *E2F* transcription factor 1, *L3MBTL1* histone methyl-lysine binding protein, *geminin* DNA replication inhibitor, *MYB* proto-oncogene like 2, *p21/cyclin* dependent kinase inhibitor 1A

acid, *c-myb* and *MYCN* expression levels decrease during the differentiation stage of neuroblastoma cells (14-18). In humans, *c-myb*, *MYB proto-oncogene like 2* (*B-myb*) and *MYB proto-oncogene like 1* (*A-myb*) belong to the *myb* gene family, and contain highly-conserved N-terminal domains (19). The functional orthologs *B-myb* and *Drosophila melanogaster-myb* (*Dm-myb*) share essential conserved functions required for cell proliferation, whereas the paralogous genes, *A-myb* and *c-myb*, have acquired novel functions (20). The *Dm-Myb* protein complex is directly involved in DNA replication and binds to amplification-control-element-on-3 (*ACE3*) and replication origin- $\beta$  in a site-specific manner (21), necessary for chorion gene amplification on the third chromosome in *Drosophila* ovarian follicle cells (22).

The *Dm-myb* complex regulates the expression of developmentally-regulated genes (23). Additionally, it has been proposed that this complex may be involved in the activation or repression of transcription and DNA replication, depending on the presence of E2F transcription factor 1 (E2F1) or E2F transcription factor 2 (E2F2) with other particular cofactors, respectively. *Drosophila* lethal (3) malignant brain tumor [*D-L(3)mbt*] protein has also been associated with the *Myb-MuvB* repressor complex (23).

The human homolog of *D-l(3)mbt*, *L3MBTL1 histone methyl-lysine binding protein* (*L3MBTL1*), is expressed in cancer cell lines and a variety of normal human tissues (24). *L3MBTL1*, a candidate tumor suppressor in *del(20q12)* myeloid disorders, is required for normal progression of the replication fork, and interacts with the minichromosome maintenance complex component 2-7, cell division cycle 45 and proliferating cell nuclear antigen components of the DNA replication machinery (25).

Chromatin licensing and DNA replication factor 1 (*hCdt1*) is an essential factor of the pre-replication complex and is inhibited by geminin (*GMNN*) protein to prevent re-replication during the S, G<sub>2</sub> and M phases of the cell cycle (26). *GMNN* and *hCdt1* are overexpressed in tumors and a variety of cancer-derived cell lines (27-29).

*MYCN* transcriptionally activates the *p53* tumor suppressor gene to induce apoptosis (30); however, *MYCN* suppresses the *cyclin dependent kinase inhibitor 1A* (*p21*) gene, resulting in anti-apoptotic activity of neuroblastoma (31). *MYCN* overexpression sensitizes *MYCN*-amplified neuroblastoma cells to apoptosis via the induction of *p53* (32). In addition, E2F-regulated *B-myb* and *c-myb* expression are elevated by apoptotic stimuli, causing neuronal death (33).

In the present study, potential *c-Myb* target genes, and the effect of *c-myb* RNA interference (RNAi) on *MYCN* expression and amplification in neuroblastoma were investigated. For this, a plasmid vector-mediated RNAi method with a short hairpin RNA (shRNA) directed against *c-myb* mRNA was used in *MYCN*-amplified neuroblastoma cell lines. The present study demonstrated that *c-myb* may induce the expression of *E2F1* and *L3MBTL1* and that *E2F1* may be associated with the induction of *MYCN*, *B-myb*, *p21* and *hCdt1* expression, in addition to the repression of *GMNN*. In addition, the results demonstrated that *MYCN* gene copy number was increased following treatment with *c-myb* RNAi. These findings revealed that *c-myb* is involved in controlling *MYCN* expression and amplification in *MYCN*-amplified

neuroblastoma cell lines. Following *c-myb* RNAi treatment, *L3MBTL1* expression was completely silenced, whereas *GMNN* was upregulated; the results indicate G<sub>2</sub>/M arrest. Consequently, the present study demonstrated that the *MYCN* gene may be amplified during S phase, which may occur via a replication-based mechanism.

## Materials and methods

**Sequence comparison.** The DNA sequences encompassing the *D. melanogaster-ACE3* element and that upstream of human *MYCN* were compared using the LFASTAn alignment program (version 2; bioinfo.hku.hk/services/analyseseq/cgi-bin/lfastan\_in.pl). The DNA sequences of *D. melanogaster*-chorion gene cluster (GenBank accession no. X02497.1) and *Homo sapiens*-chromosome 2 genomic contig, including the *MYCN* gene (NCBI reference sequence NT\_005334.16; region, 8493966-11135164) were downloaded from the NCBI website (ncbi.nlm.nih.gov).

**Transcription factor binding site search.** Transcription factor binding sites upstream (-1,021 to -143), including the enhancer and proximal promoter of *MYCN* gene were investigated using the TFSEARCH program (version 1.3; cbric.jp/research/db/TFSEARCH.html). In addition, the location information of the regulatory transcription factor binding sites in the promoters of all genes investigated in the present study was obtained from Qiagen, Inc. (Valencia, CA, USA) as predicted by Text Mining Application (SABioscience Corporation; Qiagen, Inc.) and the University of California Santa Cruz (UCSC) Genome Browser (sabiosciences.com/chipqpcsearch.php?app=TFBS).

**Cell culture.** Kelly (no. ACC 355), IMR32 (no. ACC 165), SIMA (no. ACC 164), MHH-NB-11 (no. ACC 157) and SH-SY5Y (no. ACC 209) cell lines were purchased from the Leibniz Institute DSMZ-German Collection of Microorganisms and Cell Cultures GmbH (Braunschweig, Germany). Kelly, SIMA and MHH-NB-11 cells were cultured in RPMI-1640 (cat. no. FG1215; Biochrom AG; Merck KGaA, Darmstadt, Germany) supplemented with 10% fetal bovine serum (cat. no. S0113; FBS; Biochrom AG; Merck KGaA), 2 mM L-glutamine, 100 U/ml penicillin and 100  $\mu$ g/ml streptomycin. In addition, the culture medium of MHH-NB-11 cells included 1X non-essential amino acids. IMR32 cells were cultured in RPMI-1640 (Biochrom AG; Merck KGaA) supplemented with 20% FBS, 2 mM L-glutamine, 100 U/ml penicillin, 100  $\mu$ g/ml streptomycin and 1X non-essential amino acids. SH-SY5Y cells were cultured in Dulbecco's modified Eagle's medium (cat. no. FG0415; DMEM; Biochrom AG; Merck KGaA) supplemented with 20% FBS, 2 mM L-glutamine, 100 U/ml penicillin and 100  $\mu$ g/ml streptomycin. Cells were incubated at 37°C in a humidified atmosphere containing 5% CO<sub>2</sub>.

**Fluorescence in situ hybridization (FISH).** FISH was performed as previously described (3,34). In FISH experiments, *MYCN* gene (2p24)/Chromosome 2  $\alpha$ -Satellite (red/green; cat. no. PONC0224; Qbiogene, Inc.; Thermo Fisher Scientific, Inc., Waltham, MA, USA), 1p36/Chr 1 SE

(Poseidon probe red/green, cat. no. KB-10705; Kretech Diagnostics Corp., Amsterdam, LG, Netherlands) and 1p36/1q25 (Vysis probe orange/green, cat. no. 32-231004; Abbott Pharmaceutical Co. Ltd., Lake Bluff, IL, USA) probes were used.

Neuroblastoma cells were seeded into 25-cm<sup>2</sup> tissue culture flasks and grown in culture medium specific for each cell line (please see 'Cell culture' section for the characteristics of each growth medium) in a humidified atmosphere containing 5% CO<sub>2</sub> at 37°C. The cells were detached with trypsin-EDTA (Biochrom AG; Merck KGaA) and incubated with 80 µl colcemid (Biological Industries, Kibbutz Beit Haemek, Israel) in a tube containing 5 ml culture medium in a 37°C water bath for 30 min. Following centrifugation at 300 x g for 10 min at room temperature, the cell pellets were incubated with 8 ml hypotonic solution (0.075 M) (Biochrom AG; Merck KGaA) in a 37°C water bath for 30 min. For the fixation of the cell pellets, 5 ml fresh Carnoy's solution (3:1 Methanol:Glacial Acetic Acid; Merck KGaA) was used for 2-3 min at room temperature followed by centrifugation at 300 x g for 10 min (repeated five times).

The homogenized cells were dropped onto slides, and a 2X SSC (AppliChem GmbH, Darmstadt, Germany)/0.5% NP-40 (AppliChem) mixture was used for washing the slides in a 37°C water bath for 30 min. The slides were dehydrated in an ethanol (AppliChem) series of 70, 85 and 96%, respectively. The double-stranded DNAs on the slides were denatured in 70% formamide (AppliChem)/2X SSC (AppliChem) at 70°C for 2 min (5 min for Abbott/Vysis 1p36 probe). The denaturation of probes was performed in a 96°C water bath for 5 min (5 and 10 min at 75°C for Vysis and Poseidon 1p36 probes, respectively). The DNAs were hybridized with the probes via overnight incubation at 37°C in a hybridization box. The 0.5X SSC (AppliChem)/0.1% SDS (Honeywell Riedel-de Haën AG, Seelze, Germany), 1X PBD including NP40 (AppliChem) and Tween 20 (Santacruz Biotechnology, Inc., Dallas, Texas, USA) and 70% ethanol (AppliChem), respectively, were used for washing the slides after hybridization overnight. Cell nuclei were counterstained with 4',6-diamidino-2-phenylindole II (DAPI II; cat. no. 30-804841; Abbott Pharmaceutical Co. Ltd.) suspended in an antifade solution.

FISH slides were analyzed under an epifluorescence microscope (magnification, x100; Nikon Eclipse E600, Nikon Corporation, Tokyo, Japan) equipped with DAPI, FITC, rhodamine and triple band-pass filter sets. FISH images from interphase nuclei and metaphase spreads were captured using a high-sensitivity monochrome charge-coupled device camera, which was integrated with a Macintosh computer and processed with MacProbe imaging software (version 4.0, PSI Scientific Systems, League City, TX, USA).

In FISH analyses, 2 red and 2 green signals for *MYCN* and internal control per diploid genome were considered normal; 3-5 red signals vs. 2 green signals per diploid genome were scored as a low copy number of the *MYCN* gene; 6-10 red signals vs. 2 green signals per diploid genome were scored as an intermediate copy number of *MYCN* gene, whereas >10 red signals vs. 2 green signals per diploid genome indicate high copy number of *MYCN*.

For 1p36 and the internal control, 2 orange/red and 2 green signals per diploid genome were considered normal. Only 1 orange/red signal vs. ≥2 green signals per diploid genome was classified as a 1p36 deletion. A total of 2 orange/red signals vs. 3 green signals per diploid genome and so forth (representing at least one more signal number of control than that of the 1p36 probe) were considered to indicate an imbalance in 1p36 copy number; 3 orange/red and 3 green signals per diploid genome were classified as a 1p36-3/3 balanced alteration.

**DNA extraction.** Kelly, SIMA, IMR32, MHH-NB-11 and SH-SY5Y cells were seeded into 75-cm<sup>2</sup> tissue culture flasks and grown in a culture medium until cells reached near-confluence in a humidified atmosphere containing 5% CO<sub>2</sub> at 37°C. Genomic DNA was extracted using phenol:chloroform:isoamyl alcohol (25:24:1, respectively), pH 8.0 (cat. no. A0889.0500; AppliChem GmbH, Darmstadt, Germany) as previously described (35).

**cDNA synthesis.** Kelly, SIMA, IMR32, MHH-NB-11 and SH-SY5Y cells were seeded into 24-well plates at a density of 4x10<sup>4</sup> cells in 0.75 ml culture medium per well and grown in a culture medium until cells reached near-confluence in a humidified atmosphere containing 5% CO<sub>2</sub> at 37°C. First-strand cDNAs were synthesized directly from adherent cultured cells, without requiring RNA purification or RNase H digestion steps, using the FastLane Cell cDNA kit (cat. no. 215011; Qiagen, Inc.) according to the manufacturer's protocol. The procedure of this kit involves four steps: i) removing extracellular contaminants, ii) performing cell lysis and RNA stabilization, iii) eliminating genomic DNA and iv) producing the first-strand cDNA via reverse transcription. This kit has been optimized for use particularly in real-time, two-step reverse transcription-quantitative polymerase chain reaction (RT-qPCR). The genomic DNA from the FastLane lysate was eliminated using gDNA Wipeout Buffer at 42°C for five min. The lysate was placed immediately on ice. The reverse-transcription reaction was performed at 42°C for 30 min; later reverse transcriptase enzyme was inactivated for finishing reaction at 95°C for three min according to the manufacturer's protocol.

**Reverse transcription-quantitative polymerase chain reaction (RT-qPCR).** In neuroblastoma cell lines, the expression levels of *c-myc* and potential target genes, and *MYCN* gene copy number compared with hypoxanthine phosphoribosyltransferase 1 (*HPRT1*) and *p53* reference genes, respectively, were determined via qPCR on a LightCycler® 2.0 instrument (Roche Diagnostics, Basel, Switzerland). Relative quantitative qPCR experiments were performed using the LightCycler® TaqMan® Master kit (cat. no. 04535286001; Roche Applied Science, Penzberg, Germany) with prevalidated hydrolysis probes, Universal ProbeLibrary Set, Human (cat. no. 04683633001; Roche Applied Science) and primers according to the manufacturer's protocol.

Probe and primer sets were designed using the web-based ProbeFinder software (version 2.40) via the UPL assay design center ([www.universalprobelibrary.com](http://www.universalprobelibrary.com)). Primer pairs were



Table I. Probe and primer pairs used for quantitative polymerase chain reaction.

A, mRNA				
NCBI accession number	Probe catalogue number	Right primer (5'-3')	Left primer (5'-3')	Amplicon size (nt)
<i>A-myb</i> BC101186.1	2, 04684982001	aagcaagtggctgggaca	ctcctttaagaatgcgcttg	75
<i>B-myb</i> X13293.1	26, 04687574001	gccagagacttccggacttt	cccagaagcagaagagga	68
<i>c-myb</i> M15024.1	62, 04688619001	agctgcatgtgtgttctgt	tgctcctaagtcaaccgaga	72
<i>MYCN</i> BC002712.2	55, 04688520001	cctcttcacatcttcacatctg	ccacaaggccctcagtacc	68
<i>E2F1</i> BC050369.2	5, 04685024001	ctgggtcaaccctcaag	tccaagaaccacatccagt	75
<i>E2F2</i> BC053676.1	68, 04688678001	gccttgacggcaatcact	ggacaaggccaacaagagg	93
<i>CDK2</i> BC003065.2	50, 04688112001	cagaatctccagggaatagg	cctcctgggtgcaata	104
<i>GMNN</i> AF067855.1	53, 04688503001	ccagaggttcaccattcagtc	aactggcagaagtagcagaaca	72
<i>hCdt1</i> AB053172.1	10, 04685091001	agcaggtgcttctccatttc	gcggagcgtctttgtgtc	117
<i>L3MBTL1</i> BC039820.1	82, 04689054001	ttccttctcttctgttccca	agcgagggaataaccagag	72
<i>p21</i> BC000275.1	70, 04688937001	agctgctcgtctgccact	ccgaggcactcagaggag	112
<i>p53</i> AB082923.1	12, 04685113001	cccttttggacttcaggtg	aggccttggaactcaaggat	85
<i>p27</i> BC001971.1	1, 04684974001	cgggttaactcttcgtggtc	agatgtcaaactgctcgagt	130
<i>HPRT1</i> BC000578.2	73, 04688961001	cgagcaagacgttcagtcct	tgacctgatttatttgcatacc	102
B, DNA				
NCBI accession number	Probe catalogue number	Right primer (5'-3')	Left primer (5'-3')	Amplicon size (nt)
<i>MYCN</i> Y00664.1	36, 04687949001	ggcctttagggcagacaga	tgaccagggtcatgcaacta	60
<i>p53</i> U94788.1	23, 04686977001	ctctagccaagcttccatcc	ttcagctcgggaaaatcg	88
<i>B-myb</i> , <i>MYB</i> proto-oncogene like 2; <i>A-myb</i> , <i>MYB</i> proto-oncogene like 1; <i>c-Myb</i> , transcriptional activator <i>Myb</i> ; <i>MYCN</i> , <i>MYCN</i> proto-oncogene <i>bHLH</i> transcription factor; <i>E2F1</i> , <i>E2F</i> transcription factor 1; <i>E2F2</i> , <i>E2F</i> transcription factor 2; <i>CDK2</i> , cyclin dependent kinase 2; <i>GMNN</i> , <i>geminin</i> ; <i>hCdt1</i> , <i>chromatin licensing and DNA replication factor 1</i> ; <i>L3MBTL1</i> , <i>L3MBTL1</i> histone methyl-lysine binding protein; <i>p21</i> , cyclin-dependent kinase inhibitor 1A; <i>p27</i> , cyclin-dependent kinase inhibitor 1B; <i>HPRT1</i> , hypoxanthine phosphoribosyltransferase 1.				

synthesized by Gene Link, Inc. (Hawthorne, NY, USA). NCBI accession numbers, probe/primer sets and amplicon sizes are presented in Table I.

In the calculation of both mRNA expression levels and gene copy number in neuroblastoma cell lines, the following equations ( $\Delta C_p$  method) were used: Presumed as  $E=2$ ,  $\Delta C_p = (C_{p_{target}} - C_{p_{reference}})$  and  $R = 2^{-\Delta C_p}$  (36). A heatmap for visualizing gene expression and *MYCN* gene copy number within neuroblastoma cell lines was produced using Heatmapper software (www.heatmapper.ca) (37).

In addition, *MYCN* copy number and gene expression levels from *MYCN*-amplified neuroblastoma cell lines prior to- and post-treatment with *c-myb* RNAi as normalized to the  $C_p$  values of target and reference genes of SH-SY5Y cells, were determined using the following equation ( $\Delta\Delta C_p$  method): Presumed as  $E=2$

$$R1 = 2^{-\Delta\Delta C_p} = 2^{-[\Delta C_{p_{target}}(sample-control) - \Delta C_{p_{ref}}(sample-control)]} \quad (36).$$

In the efficiency-corrected (dilution) method, to determine the slope ( $S$ ), the standard curves were produced between mean  $C_p$  values and logarithms (logs) of five serial starting template concentrations (ranging from 2-32 ng) using Excel (v. 2; Turkish, Home and Student version/initial release date; 07/17/2007, Microsoft Corporation, Redmond, WA, USA).

$E$  and  $R2$  values were calculated using the following equations:

$$E_{target \text{ or } ref} = 10^{\frac{-1/S}{\Delta C_p}} \text{ and } R2 = \frac{(E_{target})^{\Delta C_{p_{target}}(control-sample)}}{(E_{ref})^{\Delta C_{p_{ref}}(control-sample)}} \quad (36,38).$$

**RNAi.** In the *MYCN*-amplified Kelly, SIMA, IMR32 and MHH-NB-11 cell lines, *c-myb* mRNA expression was dysregulated using a specific shRNA-expressing pre-made plasmid DNA vector (custom-made psiRNA-h7SKneo G1 kit; cat. no. ksirna3-n21; InvivoGen, San Diego, CA, USA) according to the manufacturer's protocols.

A shRNA insert in the double-stranded RNA structure, which specifically targeted *c-myb* mRNA (NCBI accession no. M15024.1), was designed using InvivoGen siRNA wizard software (version 2.4; sirnawizard.com) and later ligated into the psiRNA-h7SKneo G1 expression vector. Pre-made plasmid DNA vectors (InvivoGen) expressing shRNAs for enhanced green fluorescent protein (EGFP) or irrelevant genes served as shRNA controls. Plasmid vectors containing the sequences of shRNA targeting *c-myb* mRNA and control shRNAs were transformed into *E. coli* LyoComp GT116 strain (InvivoGen).

For *SpeI* enzyme digestion and DNA sequencing, plasmid DNA was extracted from transformed cells using the High

Pure Plasmid Isolation kit (Roche Applied Science, Penzberg, Germany) according to the manufacturer's protocols. Plasmid DNA vector expressing the shRNA directed against *c-myb* mRNA and EGFP control vector were cut with the *SpeI* restriction enzyme (cat. no. ER1252; Thermo Fisher Scientific, Inc.) at a concentration of 10 U/ $\mu$ l (final concentration 0.5 U/ $\mu$ l) incubated in a 37°C water bath for 14 h and imaged following agarose gel electrophoresis (1%) stained with ethidium bromide. DNA Marker II was used for genomic DNA analysis (cat. no. SM0351; Fermentas; Thermo Fisher Scientific, Inc.). The shRNA sequences of *c-myb* and EGFP vectors were confirmed by plasmid DNA sequencing (Macrogen, Inc., Seoul, Korea) in both directions using forward (OL559) and reverse (OL408) primers. Primer sequences: OL559 primer (forward) 5'-CGATAAGTAACTTGACCTAAGTG-3' and OL408 primer (reverse) 5'-GCGTTACTATGGGAACATAC-3'; *c-myb* shRNA, oligo 1 (forward) 5'-ACCTCGGTTATCTGCAGGAGTCTTCATCAAGAGTGAAGACTCCTGCAGATAACCTT-3' and oligo 2 (reverse) 5'-CAAAAAGGTTATCTGCAGGAGTCTTCACCTCTTGATGAAGACTCCTGCAGATAACCG-3'; EGFP shRNA, oligo 1 (forward) 5'-ACCTCGCAAGCTGACCCTGAAGTTCACACCTGAACCTCAGGGTCAGCTTGCTT-3' and oligo 2 (reverse) 5'-CAAAAAGCAAGCTGACCCTGAAGTTCAGGTGGTGAACCTCAGGGTCAGCTTGCG-3'.

For stable transfection, purified plasmid DNA was isolated in intermediate quantities using the Genopure Plasmid Midi kit (Roche Applied Science). LyoVec reagent (InvivoGen) was used for the transfection of plasmid DNAs (5–6  $\mu$ g) into *MYCN*-amplified neuroblastoma cell lines [cell number per well (6-well plate):  $8 \times 10^5$ ]. Selection and maintenance of transfected cells expressing the neomycin-resistance (*neo*) gene were performed with G418 treatment (InvivoGen) at a concentration of 500–800  $\mu$ g/ml for 4 weeks.

**Statistical analysis.** Statistical differences were determined using a one-tailed Wilcoxon signed-rank test. For two-tailed analysis, Spearman's ( $r_s$ ) and Pearson's ( $r$ ) coefficients were used to investigate correlation; correlation coefficients ( $r$ ,  $r_s$ ) were evaluated according to the classified criteria as low (0.00–0.24), moderate (0.25–0.49), strong (0.50–0.74) and very strong (0.75–1.00) (39).  $P < 0.05$  was considered to indicate a statistically significant difference. All analyses were performed using SPSS software version 11.0 (SPSS, Inc., Chicago, IL, USA).

## Results

**Sequence upstream of human *MYCN* gene shares ~44% sequence identity with a region encompassing *ACE3*, upstream of chorion genes in *D. melanogaster*.** It has been determined that promoter and enhancer regions are located ~200 and 800 bp upstream of *MYCN*, respectively, and have been reported to be responsible for basal and cell type-specific expression in a variety of murine and human cell lines (40). In addition, the similar organization of the origin elements and replicators, including *ACE3* and *DHFR*, from *Drosophila*, mammals, *Tetrahymena* and *Sciara* has been reviewed previously (41). In normal human cells, amplified DNA has not been observed at frequencies greater than  $1/10^8$ , and *MYCN*

expression has been reported to be limited in normal human adult tissues (42,43).

Taken together, previous reports have suggested that certain *trans*-acting and epigenetic factors may serve important roles in the transcriptional and/or epigenetic control of *MYCN* expression and amplification. It was hypothesized that the DNA sequences of upstream *cis*-regulatory elements of amplifiable genes in a variety of organisms may be evolutionarily conserved, at least in part. The present study thus investigated the degree of sequence similarity between sequence upstream of the human *MYCN* gene and the *ACE3* element controlling chorion gene amplification in *D. melanogaster* (44).

Initially, the DNA sequences encompassing *MYCN* upstream and *ACE3* were compared using the LFASTAN program (Fig. 1A). The results revealed that sequences upstream of the human *MYCN* gene (–1,021 to –143; bases 2,466,909 to 2,467,787), including the enhancer and proximal promoter, share a 43.545% sequence identity in an overlap of 914 nucleotides with a DNA fragment (bases 14 to 884) spanning the *D. melanogaster ACE3* sequence. This result suggested that the expression and/or amplification mechanisms of developmentally-regulated genes may be conserved among various organisms during the evolutionary process.

**Putative *c-Myb* and *E2F1* binding sites detected in the enhancer and proximal promoter located upstream of *MYCN*.** Enhancer (–980 to –860), inhibition (–860 to –797) and promoter (–279 to +108) regions of *MYCN* were previously identified in IMR32 cells (45). Additionally, *MYCN* expression mediated by this enhancer is induced at higher levels within IMR32 cells than in HeLa cells, indicating cell type-specific enhancement of *MYCN* expression. Recently, it was reported that the DNA binding motif of MYB (*c-Myb*) is specifically enriched in low-complexity transcription factor binding site (TFBS)-clustered regions (46), which suggested that *c-Myb* may contribute to cell type-specific transcriptional regulation.

To identify the putative transcription factor binding sites upstream of *MYCN*, the TFSEARCH program was employed (Fig. 1B). A total of two *c-Myb* and three *E2F1* binding sites were identified in the enhancer and proximal promoter located upstream of *MYCN*, which shares partial sequence identity with a region encompassing *ACE3*. The bioinformatics data analysis of the present study indicated that *c-Myb* and *E2F1* may be involved in the expression of the *MYCN* gene in neuroblastoma cells.

***MYCN* amplification status, *1p36* alterations and ploidy level determined by FISH analysis in neuroblastoma cell lines.** To determine *MYCN* amplification status and *1p36* alterations in neuroblastoma cells (Fig. 2), interphase nuclei and metaphase spreads were analyzed using FISH. The degree of *MYCN* amplification (>10 copies per nucleus) was notably high in Kelly, SIMA, MHH-NB-11 and IMR32 cells (Table II); however, the fluorescence signal intensity of nuclei for each *MYCN*-amplified cell line differed (Fig. 2B). The SH-SY5Y cell line lacking *MYCN* amplification most commonly included three copies (93.1%) of *MYCN* (Table II and Fig. 2B). Our recent study demonstrated that three copies of *MYCN* in SH-SY5Y may be due to an unbalanced translocation involving the *MYCN* locus at 2p24 (34). The FISH analysis



Sequence comparison between *MYCN* upstream and *ACE3*

Query	20	30	40	50	60	70	470	480	490	500	510	520
Query	CAGTTTGGAAAGTGGAAACGGTTGTGTTTATAATTTATTGTAATTTATCTCAATTTT						GGCCTCTGCCTG-GATCTGGTATAAAACA-AAACATTGGGOCAGAATAAGACATTAGTT					
Query	X::::::X	:	:	:	:	:	:	:	:	:	:	:
Query	CAGTTTGGAA--TCAAGCTGTT-TGAGGCGAGGCTGGGTCTCAGGAGGTGTGGACAGCAC						GTCTCTCTCCTGCTATTTTGCACTTGGGACTACCTCTCTTTGCTAATTACACAGGACGA					
	50710	50720	50730	50740	50750	50760	51180	51190	51200	51210	51220	51230
Query	80	90	100	110	120	130	530	540	550	560	570	580
Query	TTGCTTTT--GTATATAAATCTACCAACGCGAGCAATTTTCAGGOCATGCCTTGACT						ACCTTGGCATCGATCAACTAACCAAC-TCAGCCTCAGAATGATGAAGTTTATGTAAGG					
Query	TTCTCTCTGGTAAATCAGATTGGCTGCCA--TAACCTGGGGAATGTTGGCTT--T						AAC-TCCCTGCAAGGCTTGCTCAACGTGGGCTC--GGGCTCAGCTGCACAACAGCA					
	50770	50780	50790	50800	50810	50820	51240	51250	51260	51270	51280	
Query	140	150	160	170	180		590	600	610	620	630	640
Query	TCACTGTCTGAC-TGAAAAATCGGTGCAAGCTCTGGCAACGCT-GGGGAAAGCAACTG						-TTAAGTCCAATATGTGTTCACTCAAC-ACCTCACTGCGTCCAGTA-TGATCCTTTT					
Query	GAAAGGTTAACTTGGAGGCTGGGGAAGGCTGCAGGGAAAGTACGCCATTCCCTCTA						GTCAAAGCGGGGCTGGGTAGAAGCATCGGCTCTCCCTCC--CCAACACACACCCCGG					
	50830	50840	50850	50860	50870	50880	51290	51300	51310	51320	51330	51340
Query	190	200	210	220	230	240	650	660	670	680	690	700
Query	CAATACTGATCGAAACTATGCGGATCGGAGCGAAGAGTCAATG-CGGTGGGAATCTTA						AATAAAATATAACTACATATTATAATTAATTGAAATAATATGATTGGATC-TTCTTTTC					
Query	GGAAGCAGAGCAGGC---CGCCTCTCCTCGCGAGTGGTGGAGGAGCGCTGCAGACGTCC						AGCCTCTCGTAATTTTTTTTCTTTTAAAGCAAGCAAT-TGCCAGGCTCGCAGGCTGGG					
	50890	50900	50910	50920	50930		51350	51360	51370	51380	51390	51400
Query	250	260	270	280	290	300	710	720	730	740	750	760
Query	CGTAATGG-GTCTGCTCTCTGGTAGAAGATGGGTAAGCAGAGCGCTGCTA--TCTGG						TAATGCACCTCA-GGCTATACCCAAATTAATTGAATTTTTCTTGAATCCCTTAGTGAT					
Query	CGCGGGGGGGGGGGGAGAGCTGGGGA--GTGGCGCACTCCAGGTCGCGGCAAGGCGGG						TGCTGCATTGCACGCT---CGGCGCGAGCTGGTCTCAGAGTGCAGGC---GGTGCA-					
	50940	50950	50960	50970	50980	50990	51410	51420	51430	51440	51450	
Query	310	320	330	340	350		770	780	790	800	810	820
Query	ACCGGCGCGAATTGAGAGCGAGCATTTTGGCAGTG-CGAGATTGGGC----TGGCTGC						CTGCTCTGGGACATCTCTGCCGTTTGGGCAACTCTCAAGGAGTCCCGTGGGATTA					
Query	GCAGCTCGCTTTCTGCTCAGTC-TTCGGCAGGTTGCGCTTTGGGCGAAGAAACCAAC						-AGCGCGGGGTCACAAAAGGCGGGGAGGAGCACACCT--GGGCTTCCAGCTTTGACG					
	51000	51010	51020	51030	51040	51050	51460	51470	51480	51490	51500	51510
Query	360	370	380	390	400	410	830	840	850	860	870	
Query	ACGTCTCGGGGGCGGTCTCAAG-----ATTGCTGGCAAGAGGCGAGGCTGGAA						CGGTGGTGCC-----CAGTCGGTGGCTAT----GCCTACAGGTGCAGGCTGGCTGA					
Query	GGGGGGCCACCTCTGTAGCTCGCACTTATTTATTTATTTTCAAAACAAG--GGGGC						CTTCTCTCTGCAAGAAAGCAAGTGCGCTTTGGGCGGAAAGGCTTGGCGCTCCCTGA					
	51060	51070	51080	51090	51100	51110	51520	51530	51540	51550	51560	51570
Query	420	430	440	450	460		880					
Query	CTGGCTCTCGGGAAACCGGAGAGGCGAAACTTGCATCATATTGTCACGTAAAGAGTTG-						COGTTAAGGGGATC					
Query	GGCCTCTTTCTTCAATTGAAACTGGAACATCCAGAGGTCTGTGTCCTAAGGGGGGCGC						TTTATATGAAATC					
	51120	51130	51140	51150	51160	51170	51580					

*MYCN* upstream (−1021→−143, partial identical region with *ACE3*)

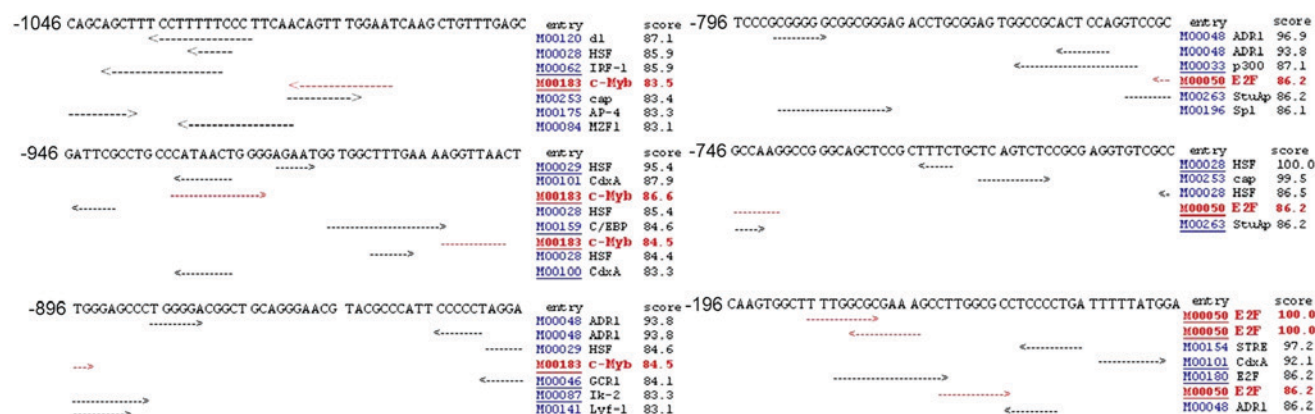


Figure 1. Sequence comparison between *MYCN* upstream and *ACE3*, and transcription factor binding sites in *MYCN* upstream. (A) A 1,020 bp DNA sequence (top; bases 1-1,020) encompassing *ACE3* from *Drosophila melanogaster* chorion gene cluster and a DNA sequence of ~65 kb (bottom) containing *MYCN* (bases 2,416,201 to 2,481,180) from human chromosome 2 genomic contig were compared using the LFASTAn program. (B) Using the TFSEARCH program, putative c-Myb and E2F1 binding sites upstream (-1,021 to -143) of human *MYCN* gene were detected. *MYCN*, *MYCN* proto-oncogene *bHLH* transcription factor; *ACE3*, *amplification-control-element-on-3*; c-Myb, transcriptional activator Myb; E2F1, E2F transcription factor 1.

In the present study, IMR32 exhibited the highest degree of 1p36 deletion, whereas the percentage was markedly low in other neuroblastoma cell lines (Table II and Fig. 2D). The 1p36 imbalance was higher in SIMA and MHH-NB-11 compared

Taken together, FISH analyses revealed that all the neuroblastoma cell lines analyzed in the present study contained aneuploid cell clones. Additionally, *MYCN*-amplified cell lines exhibited *MYCN* amplification and at least one 1p36 alteration

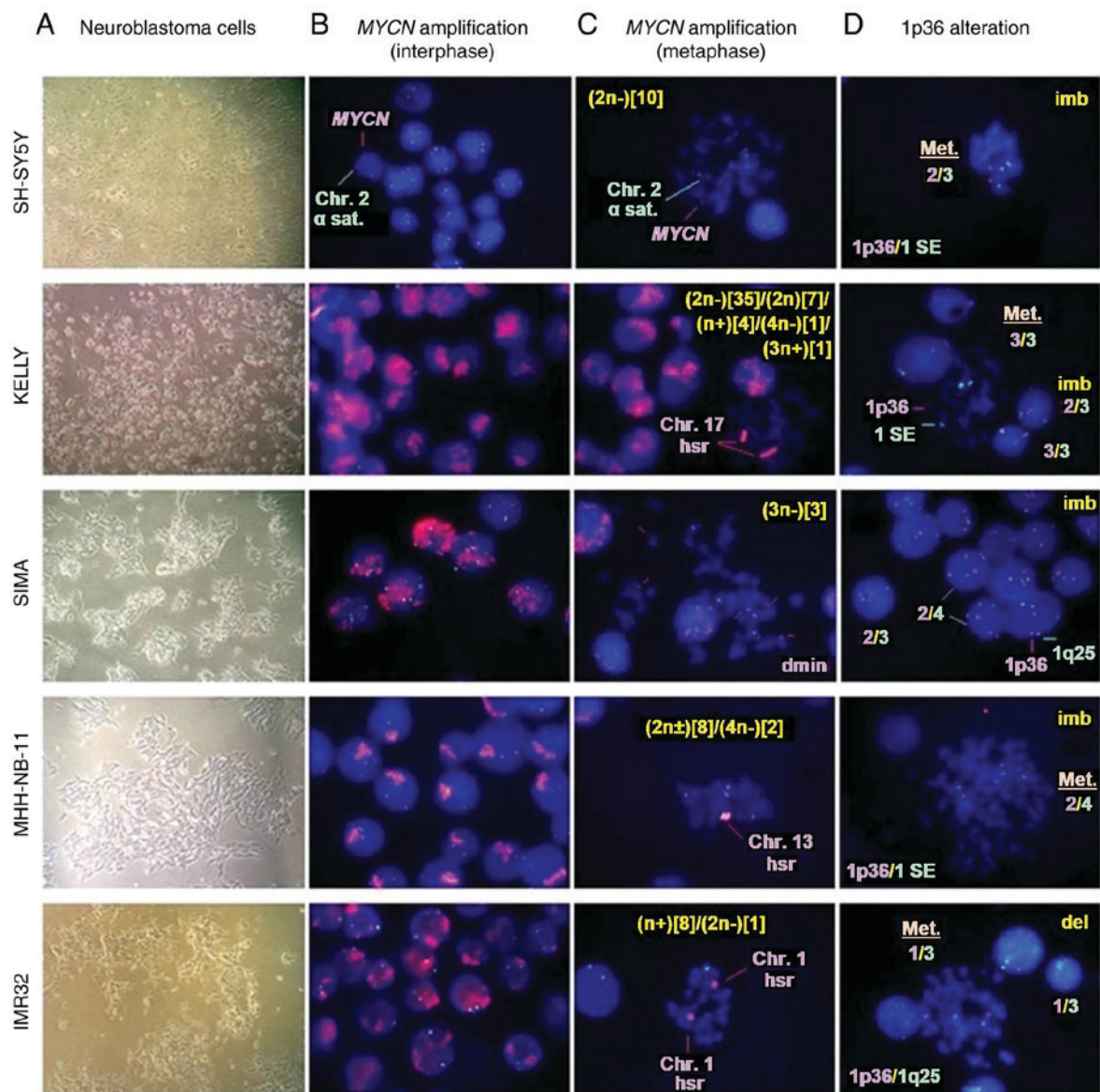


Figure 2. *MYCN* amplification and 1p36 alterations from interphase and metaphase in neuroblastoma cell lines. (A) Neuroblastoma cells were harvested for FISH experiments (magnification, x40). (B) *MYCN* amplification status of interphase nuclei was determined by FISH. (C) Modal number, hsr and dmin from metaphase in neuroblastoma cell lines are demonstrated. (D) 1p36 alterations from metaphase and interphase in neuroblastoma cell lines are presented. Magnification for B-D, x100. *MYCN*, *MYCN* proto-oncogene *bHLH* transcription factor; *ACE3*, amplification-control-element-on-3; FISH, fluorescence *in situ* hybridization; del, deletion; dmin, double minute; hsr, homogeneously staining region; imb, imbalance; SE, satellite enumeration.

as structural chromosome aberrations, whereas SH-SY5Y cells exhibited 1p36 imbalance, but no *MYCN* amplification.

*c-myb* expression, candidate target gene expression and *MYCN* gene copy number determined by qPCR in neuroblastoma cell lines. The candidate *c-Myb* target genes were selected using published literature on neuroblastoma tumor biology and gene amplification mechanisms, together with predicted binding site data for transcription factors in gene promoters (SABiosciences Text Mining Application and UCSC Genome Browser).

The present study investigated the associations between *c-myb* expression, candidate target gene expression, *MYCN* gene copy number and 1p36 alterations. *MYCN* gene copy number and the expression levels [*MYCN*, *c-myb*, *B-myb*, *A-myb*, *E2F1*, *E2F2*, *p53*, *p21*, cyclin-dependent kinase

*inhibitor 1B* (*p27*), *hCdt1*, *GMNN*, cyclin dependent kinase 2 (*CDK2*) and *L3MBTL1*] were determined in neuroblastoma cell lines compared with the reference genes, *p53* and *HPRT1*, via qPCR prior to *c-myb* RNAi (Table III and Fig. 3A). The expression levels of *MYCN* and *B-myb* were notably higher compared with those of *E2F1*, *hCdt1*, *GMNN*, *p27*, *CDK2*, *p21*, *L3MBTL1* and *c-myb* in *MYCN*-amplified cell lines (Table III and Fig. 3B).

*A-myb*, *E2F2* and *p53* were not expressed in any of the five neuroblastoma cell lines (Table III). *E2F2* has been analyzed as a candidate tumor suppressor gene located at the 1p36 locus, which is deleted in 25% of tumors and 87% of cell lines in neuroblastoma (2,10). According to FISH analysis, the 1p36 deletion was observed at a high percentage only in the IMR32 cell line (Table II), suggesting that *E2F2* may be epigenetically repressed in cell lines lacking the 1p36 deletion.



Table II. *MYCN* amplification and 1p36 alterations in neuroblastoma cell lines<sup>a</sup>.

Cell line	<i>MYCN</i> amplification (%)				1p36 alterations (%) <sup>b</sup>			
	Normal	Low	Intermediate	High	2/2	3/3 <sup>c</sup>	Deletion <sup>c</sup>	Imbalance
SH-SY5Y	3.8	96.2	0.0	0.0	67.1	2.8	0.4	28.4
Kelly	0.0	0.0	0.0	100.0	2.4	49.8	0.1	11.4
SIMA	0.0	1.5	3.4	95.1	7.4	0.9	0.4	91.1
MHH-NB-11	0.0	0.0	0.0	100.0	0.4	3.4	0.0	95.7
IMR32	0.0	0.0	0.0	100.0	5.0	0.6	85.9	8.5

<sup>a</sup>Percentage of *MYCN* amplification and 1p36 alterations from 260 and 500 interphases/metaphases using the fluorescence *in situ* hybridization method in cell lines, respectively, was determined. <sup>b</sup>1p36 alteration other than 3/3-balanced, deletion and imbalance is not presented. <sup>c</sup>Spearman's correlation coefficient, 1p36-3/3 vs. 1p36 deletion ( $r_s = -0.87$ ,  $P = 0.054$ ). *MYCN* amplification was characterized as normal (2), low (3-5), intermediate (6-10) and high (>10). *MYCN*, *MYCN* proto-oncogene *bHLH* transcription factor.

Table III. Expression of candidate *c-Myb* target genes and *MYCN* gene copy numbers in neuroblastoma cell lines.

Gene	Cell line (Cp/R)				
	SH-SY5Y	Kelly	SIMA	MHH-NB-11	IMR32
<i>MYCN</i> <sup>b</sup>	34.84±0.19/0.073	26.41±0.19/8.75	28.79±0.22/1.99	29.22±0.32/2.39	27.66±0.08/4.66
<i>B-myb</i>	28.94±0.27/4.38	27.19±0.26/5.10	28.07±0.91/3.27	27.93±0.31/5.86	27.82±0.05/4.17
<i>HPRT1</i>	31.07±0.13/1.00	29.54±0.32/1.00	29.78±0.05/1.00	30.48±0.15/1.00	29.88±0.11/1.00
<i>E2F1</i>	32.88±0.02/0.29	30.13±0.12/0.66	31.05±0.03/0.41	30.07±0.83/1.33	30.48±1.03/0.66
<i>hCdt1</i>	31.97±0.14/0.54	29.95±0.36/0.75	30.40±0.36/0.65	30.95±0.05/0.72	30.54±0.06/0.63
<i>GMNN</i> <sup>c</sup>	33.09±0.08/0.25	29.37±0.23/1.13	30.35±0.46/0.67	32.96±0.31/0.18	30.84±0.14/0.51
<i>p27</i>	33.64±0.38/0.17	29.97±0.51/0.74	32.39±0.20/0.16	31.89±0.30/0.38	30.73±0.41/0.55
<i>CDK2</i>	32.32±0.21/0.42	30.89±0.70/0.39	32.42±0.55/0.16	32.31±0.46/0.28	31.12±0.12/0.42
<i>p21</i>	34.87±0.07/0.072	32.35±0.56/0.14	35.40±0.02/0.020	37.86±0.22/0.006	32.26±0.09/0.19
<i>L3MBTL1</i>	38.83±1.16/0.005	34.99±0.71/0.023	35.17±1.61/0.024	37.17±0.81/0.010	34.52±1.29/0.040
<i>c-myb</i> <sup>b</sup>	37.54±0.85/0.011	34.59±0.84/0.030	37.18±1.08/0.006	37.18±0.20/0.010	36.11±0.12/0.013
<i>A-myb</i>	0.00	0.00	0.00	0.00	0.00
<i>E2F2</i>	0.00	0.00	0.00	0.00	0.00
<i>p53</i>	0.00	0.00	0.00	0.00	0.00

B, DNA<sup>d</sup>

Gene	Cell line (Cp/R)				
	SH-SY5Y	Kelly	SIMA	MHH-NB-11	IMR32
<i>MYCN</i> <sup>c</sup>	29.44±0.13/0.63	22.15±0.56/1488.87	24.77±0.29/80.45	23.89±0.66/74.54	24.99±0.57/82.14
<i>p53</i>	28.78±0.61/1.0	32.69±0.60/1.0	31.10±0.47/1.0	30.11±0.80/1.0	31.35±0.58/1.0

<sup>a</sup>Data (mRNA) are expressed as mean Cp ± standard error of duplicate or triplicate independent experiments in case of discordant results.

<sup>b</sup>Pearson's correlation coefficients ( $r = 0.88$ ,  $P < 0.05$ ;  $r = 0.86$ ,  $P = 0.059$ ), respectively. <sup>d</sup>The *MYCN* DNA copy number of *MYCN*-amplified cell lines was calculated from mean Cp ± standard error of the mean of ≥6 independent experiments. Using mean Cp values from quantitative polymerase chain reaction, mRNA expression and DNA copy number were determined using the  $\Delta$ Cp method. *MYCN*, *MYCN* proto-oncogene *bHLH* transcription factor; *B-myb*, *MYB* proto-oncogene like 2; *HPRT1*, hypoxanthine phosphoribosyltransferase 1; *E2F1*, *E2F* transcription factor 1; *hCdt1*, chromatin licensing and DNA replication factor 1; *GMNN*, geminin; *p27*, cyclin-dependent kinase inhibitor 1B; *CDK2*, cyclin dependent kinase 2; *p21*, cyclin-dependent kinase inhibitor 1A; *L3MBTL1*, *L3MBTL1* histone methyl-lysine binding protein; *c-Myb*, transcriptional activator *Myb*; *A-myb*, *MYB* proto-oncogene like 1; *E2F2*, *E2F* transcription factor 2.



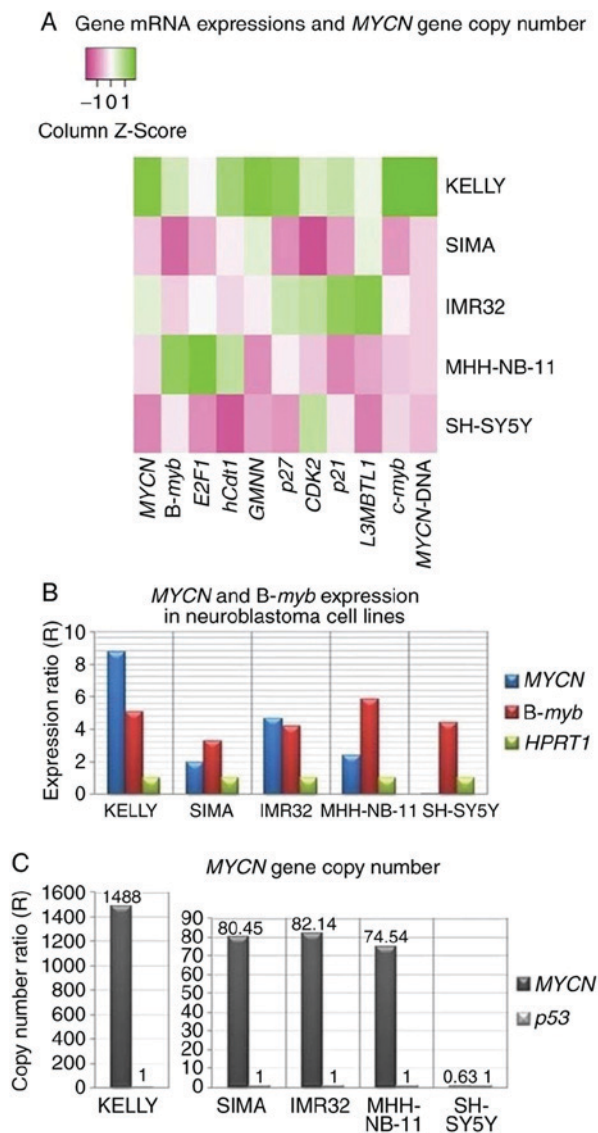


Figure 3. Expression of potential c-Myb target genes and MYCN gene copy number in neuroblastoma cell lines. (A) Heat map visualizing the mRNA expression of 10 genes and MYCN gene copy number (MYCN-DNA) from neuroblastoma cell lines compared with reference genes, *HPRT1* and *p53*, respectively. The color key represents the column Z-score of gene expression levels and copy numbers. Dark pink indicates the lowest gene expression or copy number and dark green indicates the highest gene expression or copy number. (B) Expression levels of MYCN and B-myb as compared with reference *HPRT1*; (C) MYCN gene copy number as compared with reference *p53* in neuroblastoma cell lines (see also Table III). MYCN, MYCN proto-oncogene bHLH transcription factor; B-myb, MYB proto-oncogene like 2; E2F1, E2F transcription factor 1; hCdt1, chromatin licensing and DNA replication factor 1; GMNN, geminin; p27, cyclin-dependent kinase inhibitor 1B; CDK2, cyclin dependent kinase 2; p21, cyclin-dependent kinase inhibitor 1A; L3MBTL1, L3MBTL1 histone methyl-lysine binding protein; c-Myb, transcriptional activator Myb; HPRT1, hypoxanthine phosphoribosyltransferase 1.

Using qPCR, MYCN gene copy number per haploid genome compared with the reference gene, *p53*, was notably high in Kelly cells (1,488.87 copies); however, 82.14, 80.45 and 74.54 copies were detected in IMR32, SIMA and MHH-NB-11 cells, respectively. The copy number for SH-SY5Y cells was 0.63 (Fig. 3C).

Pearson's correlation coefficient analysis revealed a notably positive significant correlation between 1p36-3/3

balanced alteration and MYCN gene copy number ( $r=0.99$ ,  $P<0.001$ ; Tables II and III, and Fig. 4A), which requires further cytogenetic examination in MYCN-amplified neuroblastoma cells bearing the 1p36-3/3 alteration. Our recent study identified a large interstitial deletion at 1q25-q41 in Kelly cell line predominantly possessing the 1p36-3/3 alteration in metaphase (34), suggesting that loss of heterozygosity of one or more tumor suppressor genes located in this region may contribute to a significant increase in MYCN gene copy number.

The mRNA expression levels of MYCN and c-myb genes declined within 3 h of treatment with retinoic acid of neuroblastoma cell lines (16). Statistical analysis revealed a significant positive correlation between c-myb and MYCN expression (Table III and Fig. 4B). This finding suggested that there may be an association between the expression of c-myb and MYCN genes in neuroblastoma cells.

**Correlations between 1p36 alterations and expression of c-myb, B-myb and p21 genes.** Previous reports have revealed that c-Myb and B-Myb facilitate G<sub>2</sub>/M progression via the direct upregulation of cyclin B1 in normal, embryonic stem and cancer cells (47-49), whereas depletion of p21 causes chromosome segregation and cytokinesis defects in HCT116, HeLa and SAOS-2 cells (50). Statistical analyses of the present study revealed a significant negative correlation between p21 expression and 1p36 imbalance ( $r_s=-1.00$ ,  $P<0.001$ ; Fig. 4C); however, a significant positive correlation between c-myb expression and 1p36-3/3 alteration ( $r=0.96$ ,  $P<0.02$ ; Fig. 4D) in neuroblastoma cell lines was observed (Tables II and III). In addition, B-myb expression and 1p36-3/3 alteration were negatively correlated with 1p36 deletion ( $r_s=-0.82$ ,  $P=0.089$ ;  $r_s=-0.87$ ,  $P=0.054$ ; Tables II and III; Fig. 4E and F). All statistical data suggested that c-myb, B-myb and p21 genes may serve an important role against the genomic instability of chromosome 1p in neuroblastoma cells.

**c-myb and E2F1 may be involved in controlling MYCN expression and amplification.** The present study employed RNAi against c-myb mRNA. A c-myb-specific shRNA sequence was designed and ligated into a plasmid DNA vector. Following transformation, plasmid DNA was transfected into MYCN-amplified Kelly, IMR32, SIMA and MHH-NB-11 neuroblastoma cell lines. To generate stably transfected cell lines, the cells expressing c-myb shRNA were selected using G418. The presence of c-myb-specific and EGFP-specific shRNAs in plasmid vectors prior to transfection was confirmed by *SpeI* enzyme digestion and DNA sequencing.

RNAi reduced c-myb mRNA expression by 95.58, 77.79, 86.42 and 88.89% in Kelly, SIMA, MHH-NB-11 and IMR32 cells, respectively (Fig. 5A). MYCN/*p53* DNA copy number ratios from MYCN-amplified cell lines were determined using the  $\Delta\Delta C_p$  method (36) as normalized to the  $C_p$  values of MYCN and *p53* genes from the SH-SY5Y control cell line in pre- and post-c-myb RNAi groups. These results were compared with those of the efficiency corrected (dilution) method (36,38) in Kelly, SIMA and IMR32 cells. The results of the present study revealed that MYCN gene copy numbers increased by 115.85, 71.70, 85.31 and 53.69% following c-myb RNAi treatment of Kelly, SIMA, IMR32 and MHH-NB-11 cells, respectively (Fig. 5B).

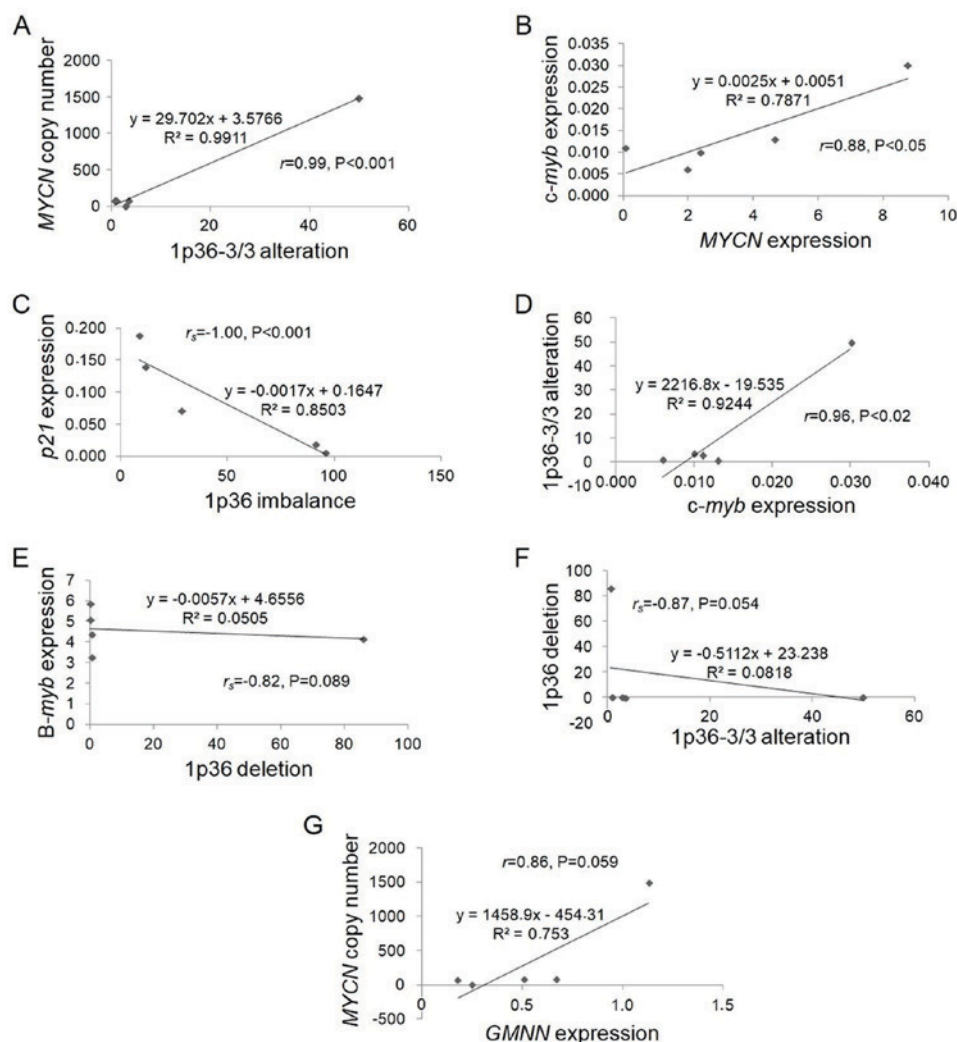


Figure 4. Scatter plots for correlations of gene expressions and genomic alterations identified in neuroblastoma cell lines. The correlations of (A) *MYCN* copy number and 1p36-3/3 alteration, (B) *c-myb* and *MYCN* expression, (C) *p21* expression and 1p36 imbalance, (D) 1p36-3/3 alteration and *c-myb* expression, (E) *B-myb* expression and 1p36 deletion, (F) 1p36 deletion and 1p36-3/3 alteration and (G) *MYCN* copy number and *GMNN* expression were presented. The scatter plots were produced using Excel. *MYCN*, *MYCN* proto-oncogene *bHLH* transcription factor; *c-myb*, transcriptional activator *Myb*; *B-myb*, *MYB* proto-oncogene like 2; *GMNN*, *geminin*; *p21*, *cyclin-dependent kinase inhibitor 1A*.

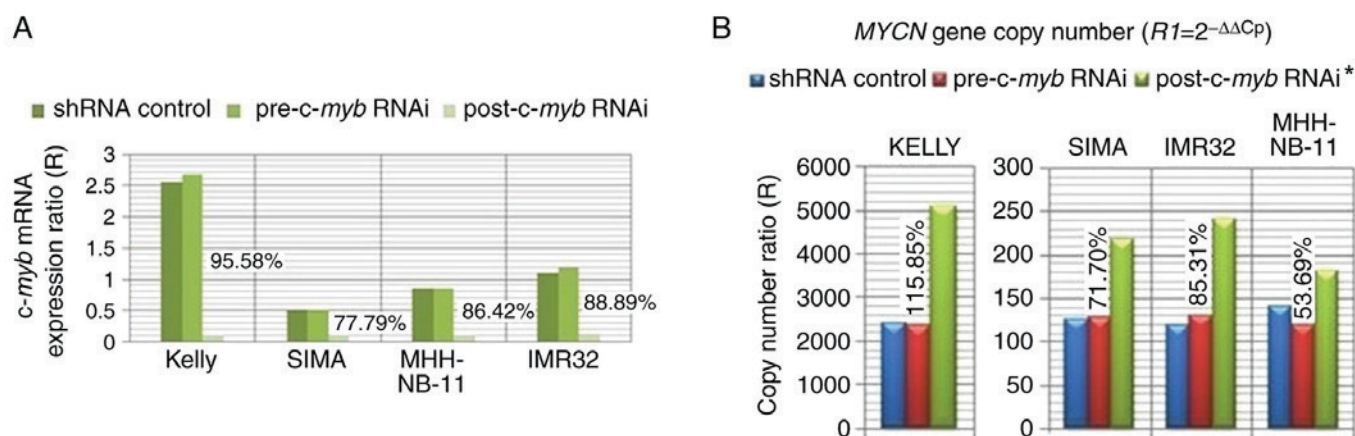


Figure 5. The effect of *c-myb* RNAi treatment on *MYCN* gene copy number. (A) Interference rate of *c-myb* mRNA was presented as compared with shRNA controls in *MYCN*-amplified neuroblastoma cell lines. The expression levels of *c-myb* mRNA were determined pre- and post-*c-myb* RNAi treatment of Kelly, SIMA, MHH-NB-11 and IMR32 cell lines, as normalized to the Cp values of target and reference genes of the SH-SY5Y control cell line. R-value was calculated using the mean Cp  $\pm$  standard error of duplicate or triplicate experiments in case of discordant results. (B) *MYCN/p53* DNA copy number ratios were determined by the delta-delta Cp method pre- and post-*c-myb* RNAi treatment as compared with shRNA control in *MYCN*-amplified neuroblastoma cell lines. Data are expressed as mean Cp  $\pm$  standard error of the mean from  $\geq 6$  independent experiments. \* $P < 0.05$ , Wilcoxon signed rank test (one-tailed). shRNA, short hairpin RNA; *c-myb*, transcriptional activator *myb*; RNAi, RNA interference; *MYCN*, *MYCN* proto-oncogene *bHLH* transcription factor.



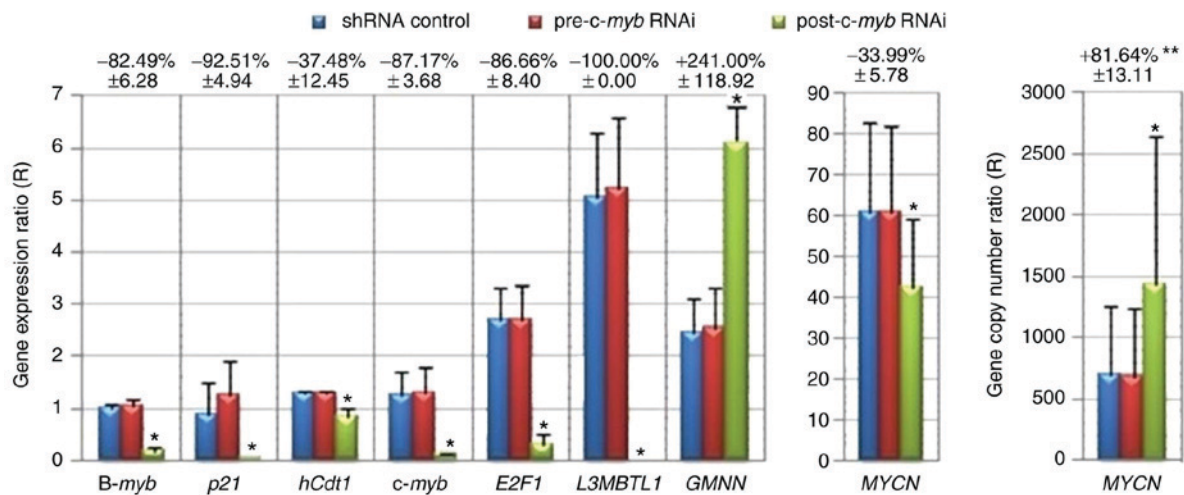


Figure 6. Alterations in potential c-Myb target gene expression and *MYCN* gene copy number following treatment with *c-myb* RNAi. *MYCN* gene copy number and expression levels of *c-myb* and potential target genes (*B-myb*, *p21*, *hCdt1*, *E2F1*, *L3MBTL1*, *GMNN* and *MYCN*) were calculated in *MYCN*-amplified neuroblastoma cell lines as normalized to the Cp values of target and reference genes of SH-SY5Y control cell line using the delta-delta Cp method (36). \*\*Data are expressed as mean variation (%) ± standard error of the mean from Kelly, SIMA, MHH-NB-11 and IMR32 cell lines (n=4). \*P<0.05; Wilcoxon signed rank test (one-tailed). shRNA, short hairpin RNA; RNAi, RNA interference; *B-myb*, *MYB* proto-oncogene like 2; *p21*, cyclin-dependent kinase inhibitor 1A; *hCdt1*, chromatin licensing and DNA replication factor 1; *c-myb*, transcriptional activator myb; *E2F1*, *E2F* transcription factor 1; *L3MBTL1*, *L3MBTL1* histone methyl-lysine binding protein; *GMNN*, geminin; *MYCN*, *MYCN* proto-oncogene bHLH transcription factor.

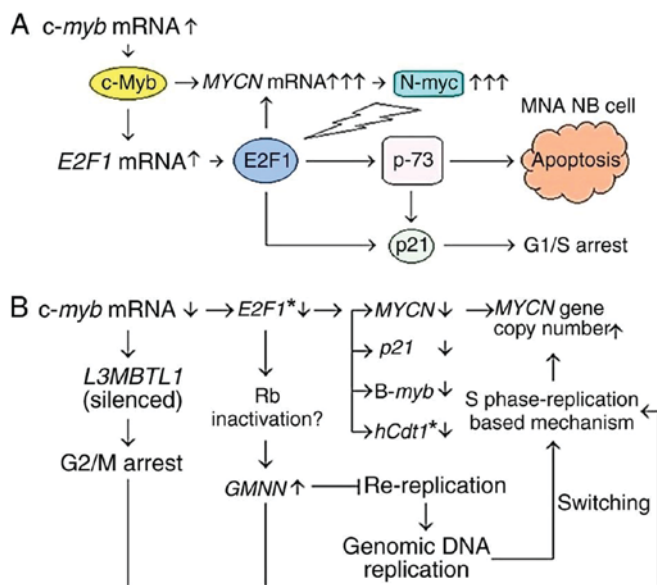


Figure 7. Involvement of *c-myb* and *E2F1* in the expression and amplification of *MYCN*. (A) Model mechanism indicates the possible contribution of *c-myb* and *E2F1* genes in the apoptotic elimination of *MYCN*-amplified neuroblastoma (MNA NB) cells via the upregulation of *MYCN* expression. *MYCN* overexpression indirectly activates the *E2F1*-induced apoptosis signaling pathway, potentially by inhibiting miR-20a and miR-92a, which prevent upregulation of *E2F* genes. (B) Flow schema showing the alterations in *MYCN* gene copy number and expression of *c-myb*, *E2F1* and potential target genes following treatment with *c-myb* RNAi in *MYCN*-amplified neuroblastoma cell lines. \*Spearman's correlation coefficient, two-tailed ( $r_s=1.0$ ,  $P<0.01$ ). miR, microRNA; RNAi, RNA interference. *c-myb*, transcriptional activator myb; *MYCN*, *MYCN* proto-oncogene bHLH transcription factor; *E2F1*, *E2F* transcription factor 1; *p-73*, tumor protein p73; *p21*, cyclin-dependent kinase inhibitor 1A; *L3MBTL1*, *L3MBTL1* histone methyl-lysine binding protein; *B-myb*, *MYB* proto-oncogene like 2; *hCdt1*, chromatin licensing and DNA replication factor 1; *Rb*, RB transcriptional corepressor; *GMNN*, geminin.

The findings of the present study suggested that *c-myb* may be involved in controlling *MYCN* amplification.

The expression levels of *MYCN*, *c-myb*, *E2F1*, *hCdt1*, *B-myb*, *GMNN*, *p21* and *L3MBTL1* genes in Kelly, SIMA, MHH-NB-11 and IMR32 cell lines as normalized to the Cp values of target and reference (*HPRT1*) genes of the control SH-SY5Y cell line were determined pre- and post-*c-myb* RNAi. The mRNA expression level of each gene was presented as the mean of related expression levels from the four aforementioned *MYCN*-amplified cell lines (Fig. 6). The expression level of *MYCN* was moderately decreased by  $33.99 \pm 5.78\%$  following treatment with *c-myb* RNAi in *MYCN*-amplified cell lines, while *E2F1* expression was downregulated by  $86.66 \pm 8.40\%$ . These results suggested that *c-myb* may be involved in the induction of *E2F1* and *MYCN* expression, potentially via putative c-Myb binding sites in their promoters.

However, the *c-myb* may also be indirectly associated with *MYCN* expression via the upregulation of *E2F1* (Fig. 7A and B). *E2F1* may be involved in activation of the *MYCN* promoter, possibly via putative *E2F1* binding sites (Fig. 1B). It was previously reported that *E2F1-3* proteins activate the *MYCN* promoter via *E2F* binding sites in Kelly and IMR32 cells (51). Taken together, the findings of the present study indicate that *c-myb* and *E2F1* may be involved in controlling *MYCN* expression and amplification in *MYCN*-amplified neuroblastoma cells.

*E2F1* may contribute to *hCdt1*, *p21* and *B-myb* gene expression in *MYCN*-amplified neuroblastoma cells. In HCT116 cells, the *hCdt1* promoter is activated by *E2F1* (52). In addition, *E2F1* induces *p21* transcription by directly binding to the proximal promoter of *p21* via a p53-independent mechanism in NIH3T3 cells (53), but also transactivates the *B-myb* promoter in SAOS-2 cells (54).

In the present study, the mRNA expression level of *hCdt1* declined by  $37.48 \pm 12.45\%$  following *c-myb* RNAi in *MYCN*-amplified neuroblastoma cell lines (Fig. 6). In addition, a significant positive correlation was identified



between *E2F1* and *hCdt1* expression post-*c-myb* RNAi. *p21* was also expressed; however, the *p53* transcript was not detected in neuroblastoma cells (Table III). Following *c-myb* RNAi treatment, *p21* expression was downregulated by  $92.51 \pm 4.94\%$  in *MYCN*-amplified neuroblastoma cell lines (Fig. 6). Additionally, *B-myb* expression was downregulated by  $82.49 \pm 6.28\%$  following *c-myb* RNAi treatment (Fig. 6).

These results suggest that *E2F1* may induce *hCdt1*, *p21* and *B-myb* expression, potentially via putative *E2F1* binding sites in the promoters of these genes in *MYCN*-amplified neuroblastoma cells (Fig. 7).

*MYCN* gene is amplified during S phase, possibly via a replication-based mechanism: *GMNN* expression is upregulated following *c-myb* RNAi treatment in *MYCN*-amplified neuroblastoma cell lines. *GMNN* transcription is induced by E2F1-4 transcription factors via the RB transcriptional corepressor 1 (Rb)/E2F signaling pathway (52). The present study reported *GMNN* upregulation; however, *E2F1* mRNA expression was downregulated following *c-myb* RNAi treatment (Fig. 6). *GMNN* was also upregulated following *E2F1* RNAi treatment (data not shown) in *MYCN*-amplified neuroblastoma cell lines.

The mRNA expression levels of *GMNN* are higher in the S and G<sub>2</sub>/M phases compared with the G<sub>1</sub>/S transition of the cell cycle (28,52). In addition, Rb serves an important role in the repression of *GMNN* via intragenic E2F sites during G<sub>1</sub> (55). The promoter of *Rb* contains a putative E2F1 binding site, suggesting that E2F1 may directly regulate the *Rb* promoter. Therefore, *E2F1* may be associated with the repression of *GMNN* expression via the induction of Rb in *MYCN*-amplified neuroblastoma cells (Fig. 7B). These findings indicate that *MYCN* gene copy number increased during S phase, while neuroblastoma cells progress toward G<sub>2</sub>/M phase following *c-myb* RNAi treatment (Fig. 7B).

*c-myb* RNAi causes silencing of *L3MBTL1* expression in *MYCN*-amplified cell lines, indicating G<sub>2</sub>/M arrest. Inhibition of *L3MBTL1* mRNA expression leads to G<sub>2</sub>/M arrest in a variety of cancerous and normal human cells (25). In the present study, *L3MBTL1* expression was silenced in *MYCN*-amplified cell lines following treatment with *c-myb* RNAi (Fig. 6). In addition, bioinformatics analysis demonstrated that the promoter of *L3MBTL1* harbors a putative binding site for c-Myb, but not for E2F. These results suggest that *c-myb* may induce *L3MBTL1* expression, possibly via a putative c-Myb binding site identified in the promoter of *L3MBTL1* in *MYCN*-amplified neuroblastoma cells (Fig. 7B).

In addition, *L3MBTL1* expression was highly downregulated by *E2F1* RNAi in Kelly, SIMA and IMR32 cells (data not shown), suggesting that E2F1 may transactivate the promoter of *c-myb* in neuroblastoma cells, similar to human glioblastoma cells (56). However, the *c-myb* promoter does not include any putative E2F binding sites.

In conclusion, the findings of the present study suggested that *L3MBTL1* may be a potential c-Myb target gene. In addition, similar to *GMNN* upregulation, the silencing of *L3MBTL1* expression following *c-myb* RNAi treatment indicates that *MYCN* gene copy number increased prior to G<sub>2</sub>/M arrest in *MYCN*-amplified neuroblastoma cell lines (Fig. 7B).

Taken together, it is concluded that *MYCN* gene is amplified during S phase, potentially via a replication-based mechanism.

## Discussion

Neuroblastoma is a common pediatric solid tumor derived from the primitive cells of the sympathetic nervous system (57). *MYCN* amplification is an important factor associated with poor prognosis in neuroblastoma (5). *MYCN* is amplified in 18-38% of reported cases (3,5-7) and in a panel of neuroblastoma cell lines (8). The mRNA expression levels of *MYCN* and *c-myb* decline within 3 h following treatment with retinoic acid in neuroblastoma cell lines (16). However, the expression and amplification mechanisms of *MYCN* require further study.

The present study investigated the potential target genes of c-Myb and the effects of *c-myb* RNAi on *MYCN* expression and amplification. *MYCN* gene copy number and mean expression levels of *MYCN*, *c-myb*, *E2F1*, *hCdt1*, *B-myb*, *GMNN*, *p21* and *L3MBTL1* genes were determined in *MYCN*-amplified neuroblastoma cell lines, which were normalized to their counterparts from the SH-SY5Y control cell line in pre- and post-*c-myb* RNAi treatment. To compare with those of the  $\Delta\Delta C_p$  method, *MYCN* gene copy numbers of Kelly, SIMA and IMR32 cells were also determined using the dilution method.

The  $\Delta\Delta C_p$  method revealed that *MYCN* gene copy number increased by 115.85, 71.70, 85.31 and 53.69% in Kelly, SIMA, IMR32 and MHH-NB-11 cells, respectively, following *c-myb* RNAi treatment. The dilution method also revealed that *MYCN* gene copy number was increased in Kelly (336.49%), SIMA (20.58%) and IMR32 (76.83%) cells normalized to target and reference *Cp* values of the control SH-SY5Y cell line. However, PCR amplification efficiency (*E*) values out of range 1.95-2.05 in the dilution method led to notable differences in the *MYCN* gene copy numbers compared with those obtained from the  $\Delta\Delta C_p$  method, particularly for Kelly and SIMA. Using the dilution method, *E* values >2.0, which are unexpected in theory, have been practically observed (36). Taken together,  $\Delta\Delta C_p$  and dilution methods demonstrated an increase in *MYCN* gene copy number following *c-myb* RNAi treatment, suggesting that *c-myb* may be involved in controlling *MYCN* amplification in *MYCN*-amplified neuroblastoma cells.

Previously, Beall *et al* (21) reported that the protein product of *D. melanogaster-myb* gene, which is closely associated with the vertebrate *myb* gene family (including A-*myb*, B-*myb* and c-*myb*) (19,20), is required for chorion gene amplification *in trans*. However, it was proposed that a Dm Myb-MuvB repressor complex, including D-L(3)mbt protein, may be involved in the repression of transcription and DNA replication (23). The paralogous human gene, c-*myb*, has acquired novel functions not possessed by the Dm-*myb* gene (20). *L3MBTL1*, a human homolog of the D-L(3)mbt protein, interacts with the DNA sliding clamp and other proteins, forming a replicative helicase complex, and is required for progression of the replication fork (25). Loss of *L3MBTL1* mRNA expression is an indicator of G<sub>2</sub>/M arrest (25). The present study reported that *L3MBTL1* mRNA expression was silenced, whereas *MYCN* gene copy number increased following *c-myb* RNAi treatment of *MYCN*-amplified neuroblastoma cell lines. Taken together with published data,

the findings of the present study suggest that *L3MBTL1* may act as a guard against arrest or abnormal forms of replication forks during *MYCN* amplification. Furthermore, the present study indicated that *MYCN* gene copy number was increased prior to G<sub>2</sub>/M arrest.

Statistical analysis revealed a notably significant positive correlation between *c-myb* and *MYCN* expression levels in neuroblastoma cells (Table III). Furthermore, the expression levels of *MYCN* were moderately decreased in *MYCN*-amplified neuroblastoma cells following *c-myb* RNAi treatment. In addition, bioinformatics analysis demonstrated that the enhancer and promoter of *MYCN* include putative *c-Myb* binding sites. The results of the present study suggest that *MYCN* may be a potential target gene of *c-Myb* and that *c-myb* may be associated with the induction of *MYCN* expression, potentially via the promoter and/or enhancer regions of *MYCN*. Upon induction by retinoic acid in human neuroblastoma cells, the mRNA expression levels of *c-myb* and *MYCN* decrease within 3 h (14-18).

Following treatment with *c-myb* RNAi, the mRNA expression levels of *E2F1* and *MYCN* decreased, whereas the *MYCN* gene copy number increased in *MYCN*-amplified neuroblastoma cells. Bioinformatics analyses demonstrated that the *MYCN* promoter includes putative E2F1 binding sites, while that of *E2F1* harbors *c-Myb* binding sites. These results suggested that *E2F1* may be a potential target gene of *c-Myb*; and *c-myb* gene is involved in the induction of *E2F1* expression potentially via a putative *c-Myb*-binding site in the *E2F1* promoter. As with *c-myb*, *E2F1* may also be associated with the induction of *MYCN* expression, potentially via E2F1 binding sites in the *MYCN* promoter. Our preliminary studies demonstrated that *MYCN* expression is downregulated by *E2F1* RNAi in Kelly and IMR32 cells (data not shown). E2F1-3 have been reported to activate the proximal promoter of *MYCN* gene in Kelly and IMR32 cells (51). Collectively, these findings suggested that *c-myb* and *E2F1* may be involved in controlling *MYCN* expression and amplification via the promoter and/or enhancer regions of *MYCN*.

In the present study, *B-myb* and *p21* were observed to be downregulated following treatment with *c-myb* RNAi. In addition, the expression levels of *B-myb* and *p21* decreased following *E2F1* RNAi treatment in Kelly, SIMA, MHH-NB-11 and IMR32 cell lines (data not shown). Bioinformatics data revealed that the *p21* promoter includes putative E2F1 binding sites without a *c-Myb* binding site (Qiagen, Inc.). These results indicated that *E2F1* may be associated with the induction of *B-myb* and *p21* mRNA expression, possibly via putative E2F1 binding sites in their respective promoters. A direct interaction causing S-phase arrest between the E2F1 transcription factor and the proximal promoter of *p21* was previously demonstrated in NIH3T3 cells (53), and E2F1 transactivates the *B-myb* promoter in SAOS-2 cells (54).

E2F1 transcriptionally activates the *Tp73* tumor suppressor that induces p53-responsive genes and apoptosis (58). The expression level of p21 protein is increased in the IGR-N-91 neuroblastoma cell line (containing mutated p53) infected with *TAp73a* recombinant adenovirus; this leads to G<sub>1</sub> arrest via a p53-independent signaling pathway (59). In *MYCN*-amplified neuroblastoma, *MYCN* transactivates *miR-17-5p*, which in turn accelerates cell cycle progression and protects cells from

apoptosis via the downregulation of p21 and BIM, respectively (60). *MYCN* overexpression sensitizes *MYCN*-amplified neuroblastoma cells to apoptosis via the induction of p53 (32). Additionally, enforced *MYCN* expression causes a significant reduction in cell viability via the apoptosis signaling pathway in SY5Y and SK-N-AS cell lines lacking *MYCN* amplification (61).

Furthermore, Guglielmi *et al* (18) reported that the mRNA expression levels of pro-apoptotic *E2F1* and *Tp73* are increased without modulating *Tp53* mRNA expression, due to the inhibition of miR-9, miR-20a and miR-92a by upregulated *MYCN* expression in SK-N-AS cells. It was concluded that *MYCN* may be required during the activation of neuroblastoma differentiation to induce apoptosis in undifferentiated cells. In addition, Guglielmi *et al* (18) reported that cell death was not observed following treatment with retinoic acid of *MYCN*-silenced LAN-5 cells (~40%) harboring *MYCN* amplification, whereas control LAN-5 cells did exhibit retinoic acid-induced apoptosis.

In the present study, *p21* was identified to be transcribed in neuroblastoma cells, whereas *p53* mRNA was not expressed under normal conditions. Taken together, the results suggested that *c-myb* and *E2F1* may contribute to the sensitization of *MYCN*-amplified cells to apoptosis by inducing *MYCN* overexpression that indirectly activates E2F1 protein, which in turn upregulates p73 and p21 in neuroblastoma (18,32,53,58,62-64). That is, *MYCN* amplification may be partially controlled via *E2F1*-induced G<sub>1</sub>/S arrest and apoptosis in *MYCN*-amplified neuroblastoma cells (Fig. 7A).

In a previous study, *c-Myc* expression was reported to be upregulated in 5-15% of the p53<sup>-/-</sup> mice cells in all the tissues examined, whereas <1% of p53<sup>+/+</sup> cells express detectable levels of *c-Myc* protein (65). Apoptotic p53<sup>-/-</sup> cells characteristically exhibit atypical chromosome morphology, abnormally amplified centrosomes, aneuploidy, *c-myc* gene amplification and elevated *c-Myc* protein levels, indicating that *c-Myc*-overexpressing cells undergo apoptosis and numerous genetically aberrant cells are eliminated by p53-independent apoptosis *in vivo* (65).

The apoptotic control mechanism proposed in the present study for *MYCN*-amplified neuroblastoma cells via *c-myb* and *E2F1*-associated *MYCN* overexpression can explain why the *MYCN* gene copy number increases despite reductions in mRNA expression levels of *MYCN* following *c-myb* RNAi treatment. In cisplatin-resistant UKF-NB-4 neuroblastoma cells with *MYCN* amplification, *MYCN* expression levels increased although no significant change was observed in the *MYCN* copy number following cisplatin treatment, suggesting that alterations in *MYCN* expression may not always be associated with variations in *MYCN* copy number (66). *MYCN* expression may be controlled by mechanisms independent from *MYCN* copy number under discrete conditions in neuroblastoma cell lines. Additional *MYCN* gene copies may also repress their own transcription. By analyzing genome-wide data of the regions that vary in copy number in humans and certain model organisms, it has been reported that genes with varied copy number in copy number variation (CNV) regions are expressed at lower and more variable levels than genes mapped elsewhere; CNVs also exert a global influence on

the transcriptome (67). Alterations in copy number of CNV regions can influence gene expression by several mechanisms, including physical dissociation of the transcription unit from its *cis*-acting regulators, modification of transcriptional control by altering chromatin structure and position, and perturbation of transcript structure (67). Additional copies of *MYCN* may also impair *MYCN* transcription due to steric hindrance for access to specific transcription factories, as previously described in a general hypothesis regarding extra copies of any gene (67,68).

In the present study, FISH analyses of the metaphase spreads from neuroblastoma cells revealed near-diploid ( $2n\pm$ ), hyperhaploid ( $n+$ ) and near-polyploid ( $3n-$ ,  $3n+$  and  $4n-$ ) aneuploidies. In addition, qPCR experiments revealed the expression of *CDK2* and *MYCN* genes in neuroblastoma cells. Centrosomes with multiple copies, abnormal structure and function have frequently been observed in the most common types of human malignant tumors and tumor-derived cell lines (69). Hyperactive *CDK2* and *MYCN* overexpression induce centrosome amplification and chromosomal instability, resulting in aneuploidy and formation of micronuclei (a precursor to aneuploidy) in *p53*<sup>-/-</sup> mouse embryonic fibroblasts and neuroblastoma cells following DNA damage, respectively (70,71). However, enhanced expression of *MYCN* without DNA damage in a neuroblastoma cell line did not cause centrosome hyperamplification and micronuclei formation (71).

Sugihara *et al* (71) predicted an increase in a fraction of the cell population with DNA contents of 8N, resulting from centrosome hyperamplification with DNA replication caused by the failure of cell division following DNA damage. However, Sugihara *et al* (71) also identified that the fraction of *MYCN*-EGFP cells with 8N did not increase compared with that of vector-EGFP cells, suggesting that *MYCN* overexpression may contribute to the apoptotic elimination of neuroblastoma cells with genomic DNA amplification and formation of micronuclei. Similarly, the apoptotic cells of *p53*<sup>-/-</sup> mice contain abnormally amplified centrosomes, aneuploidy, high levels of c-Myc expression and gene amplification (65).

Statistical analyses revealed that B-*myb* and *p21* expression are negatively correlated with 1p36 deletion and imbalance, respectively ( $r_s = -0.82$ ,  $P = 0.089$ ;  $r_s = -1.00$ ,  $P < 0.001$ ). Conversely, a significant positive correlation was identified between c-*myb* expression and 1p36-3/3 alteration in neuroblastoma cells ( $r = 0.96$ ,  $P < 0.02$ ), suggesting that c-*myb*, B-*myb* and *p21* may serve a role against genomic instability in chromosome 1p. *p21* deficiency leads to abnormal centriole replication (72), whereas *p21* overexpression rescues *p53*-deficient human tumor cells from endoreduplication and aneuploidy/polyploidy (73,74).

Following c-*myb* RNAi treatment, *L3MBTL1* expression was silenced in *MYCN*-amplified Kelly, SIMA, IMR32 and MHH-NB-11 neuroblastoma cell lines in the current study, indicating that *L3MBTL1* may be a potential c-Myb target gene. The c-*myb* gene may be involved in the induction of *L3MBTL1* expression, possibly via a putative c-Myb-binding site in the *L3MBTL1* promoter. In certain cancer cell lines, including SW480, the *L3MBTL1* transcript is markedly reduced (24). In addition, *L3MBTL1* has been considered to be a candidate tumor suppressor gene in myeloid malignancies associated with 20q12 deletions (25). Furthermore, depletion of *L3MBTL1* causes replicative stress, DNA breaks, activation

of the DNA damage response and genomic instability in human cells, and leads to G<sub>2</sub>/M arrest in a variety of cancerous and normal human cells (25). Considering the published literature, the results of the present study suggested that *L3MBTL1* may act as a tumor suppressor gene in neuroblastoma cells. Together, the results indicated that *MYCN* gene copy number increased prior to G<sub>2</sub>/M arrest, potentially following the loss of *L3MBTL1* mRNA expression on treatment with c-*myb* RNAi.

*GMNN* expression was also increased along with *MYCN* gene copy number following c-*myb* RNAi treatment in *MYCN*-amplified neuroblastoma cell lines in the current study. In addition, a positive correlation was identified between *GMNN* expression and *MYCN* gene copy number. These results suggest that *GMNN* upregulation may lead to a switch from genomic DNA replication to *MYCN* amplification by suppressing re-replication. Similarly, in the follicle cells of *Dm geminin* mutant ovaries, it was reported that a switch from general genomic endoreplication to the amplification cycles occurs during stage 10B (75). The present study also reported a partially identical region of ~44% between DNA fragments encompassing the sequence upstream of human *MYCN* gene and *ACE3* controlling chorion gene amplification in *D. melanogaster*. This finding suggested that the expression and/or amplification mechanisms of developmentally-regulated genes may be conserved among different organisms during the evolutionary process. As with c-*myb* RNAi, *E2F1* RNAi caused the upregulation of *GMNN* expression in *MYCN*-amplified neuroblastoma cell lines (data not shown). *GMNN* expression is transcriptionally repressed by the activation of Rb throughout G<sub>1</sub> (55). In view of the literature and the findings of the present study, it can be hypothesized that the *E2F1* gene may be indirectly involved in controlling *GMNN* expression via transcriptional activation of the *Rb* promoter.

In addition, the results of the present study suggested that *E2F1* contributed to the induction of *hCdt1* expression in *MYCN*-amplified neuroblastoma cells. Additionally, it was identified that an *E2F1* RNAi experiment in SIMA, as with c-*myb* RNAi, caused the downregulation of *hCdt1* expression (data not shown). The promoter of *hCdt1* is activated by E2F1 in HCT116 cells (52). Taken together, the results suggested that *E2F1* may be implicated in controlling the expression of *GMNN* and *hCdt1* genes throughout the cell cycle (Fig. 7B).

The mRNA expression levels of *GMNN* are upregulated in S and G<sub>2</sub>/M phases (28,52), followed by the degradation of geminin protein via APC/C<sup>Cdc20</sup> and mitotic spindle checkpoint during metaphase and early anaphase (26,76) in human cells. In addition, loss of *L3MBTL1* transcript leads to G<sub>2</sub>/M arrest (25). B-Myb and c-Myb contribute to the G<sub>2</sub>/M transition in normal human cells, embryonic stem cells and cancer cells (47-49).

In conclusion, the results of the present study revealed that c-*myb* and *E2F1* genes may be involved in controlling *MYCN* expression and amplification in *MYCN*-amplified neuroblastoma cells. As described in the model mechanism proposed in Fig. 7A, c-*myb* and *E2F1* may contribute to the apoptotic elimination of *MYCN*-amplified cells via the induction of *MYCN* overexpression that indirectly activates E2F1-induced apoptosis. However, it remains to be determined whether c-*myb* and E2F1 are involved in the induction



of apoptosis in *MYCN*-amplified neuroblastoma cell lines. In addition, *c-myb* may be associated with the upregulation of *L3MBTL1* (Fig. 7B). Furthermore, *L3MBTL1* may be considered as candidate tumor suppressor gene in neuroblastoma cells. The results of the present study also indicated that the cell cycle is stopped or delayed in the G<sub>2</sub>/M transition of the *MYCN*-amplified neuroblastoma cells following *c-myb* RNAi treatment (Fig. 7B). Therefore, it is concluded that *MYCN* gene is amplified during S phase, possibly via a replication-based mechanism (Fig. 7B).

In drug-resistant Chinese hamster sublines and two neuroblastoma cell lines, SK-N-BE(2) and IMR-32, the HSRs containing *DHFR* and *MYCN*, respectively, were previously demonstrated to undergo relatively rapid and synchronous replication prior to the midpoint of the S phase as observed by tritiated thymidine radioautography (77). However, there is no clear evidence on whether *MYCN* is amplified during S phase. Neuroblastoma cell lines harbor a head-to-tail tandem array in the direct orientation of DNA segments containing *MYCN* gene in amplified regions (78), suggesting that *MYCN* amplification may arise from a mechanism other than those involving breakage-fusion-bridge cycles that produce inverted duplications (79). Numerous replication-based mechanisms for the formation of *MYCN* or general gene amplification have been proposed (12,41,78,80-84).

Aygun (84) recently reported that long inverted repeats (LIRs) are significantly associated with 5' and 3' boundary regions of the amplicon units containing *MYCN* gene in 14 neuroblastoma cell lines and 42 other primary solid tumors, whose genomic data were obtained from the catalogue of somatic mutations in cancer (COSMIC database; cancer.sanger.ac.uk/cosmic/) (85). In addition, Aygun (86) previously reported a significant association between LIRs and the breakpoint regions of gross deletions in human cancers and inherited diseases. Numerous LIRs inside and outside the *MYCN* amplicon units were identified, suggesting that LIRs may extrude hairpin and cruciform structures in single- and double-stranded DNA during replication, respectively (84). The hairpin structure can form at an interrupted LIR on leading and lagging strand templates simultaneously during replication (87). The hairpin and cruciform conformations can cause replication fork stalling (87,88). In addition, a mean microhomology of 5.18 bp (range, 2-14 bp) between DNA sequences of 150 bp encompassing the 5' and 3' boundaries of the *MYCN* amplicon units has been reported (12,84). Microhomology between 0 and 15 bp indicates nonhomologous end joining, microhomology-mediated end joining, microhomology-mediated break-induced replication or fork stalling and template switching mechanisms (83,89,90). Consequently, the findings of the present study indicated that a replication-based mechanism involving LIRs in a microhomology-dependent manner may generate *MYCN* amplification during S phase. Therapeutic targeting of *MYCN* amplification during S phase may improve the prognosis of neuroblastoma patients.

## Acknowledgements

The authors would like to thank Professor Nur Olgun (Division of Pediatric Oncology, Oncology Institute, Dokuz

Eylul University, Izmir, Turkey) for purchasing the Kelly and IMR32 cell lines.

## Funding

The present study was supported by the Research Fund of Dokuz Eylul University (grant no. 2005.KB.SAG.077, to OA).

## Availability of data and materials

The datasets used and/or analyzed during the current study are available from the corresponding author on reasonable request.

## Authors' contributions

NA conceived the study, performed the experiments, analyzed the data, wrote the manuscript and prepared all figures and tables. OA supervised the project and conducted the research.

## Ethics approval and consent to participate

All the experiments were performed in established human neuroblastoma cell lines. The present study was approved by the local Ethics Committee of Clinical and Laboratory Research of the Faculty of Medicine, Dokuz Eylul University (04.10.2005/223, protocol no. 188).

## Patient consent for publication

Not applicable.

## Competing interests

The authors declare that they have no competing interests.

## References

1. Seeger RC, Brodeur GM, Sather H, Dalton A, Siegel SE, Wong KY and Hammond D: Association of multiple copies of the N-myc oncogene with rapid progression of neuroblastomas. *N Engl J Med* 313: 1111-1116, 1985.
2. Maris JM and Matthay KK: Molecular biology of neuroblastoma. *J Clin Oncol* 17: 2264-2279, 1999.
3. Altunoz O, Aygun N, Tumer S, Ozer E, Olgun N and Sakizli M: Correlation of modified Shimada classification with MYCN and 1p36 status detected by fluorescence in situ hybridization in neuroblastoma. *Cancer Genet Cytogenet* 172: 113-119, 2007.
4. Gurney JG, Ross JA, Wall DA, Bleyer WA, Severson RK and Robison LL: Infant cancer in the U.S.: Histology-specific incidence and trends, 1973 to 1992. *J Pediatr Hematol Oncol* 19: 428-432, 1997.
5. Brodeur GM, Seeger RC, Schwab M, Varmus HE and Bishop JM: Amplification of N-myc in untreated human neuroblastomas correlates with advanced disease stage. *Science* 224: 1121-1124, 1984.
6. Bartram CR and Berthold F: Amplification and expression of the N-myc gene in neuroblastoma. *Eur J Pediatr* 146: 162-165, 1987.
7. Valent A, Guillaud-Bataille M, Farra C, Lozach F, Spengler B, Terrier-Lacombe MJ, Valteau-Couanet D, Danglot G, Lenoir GM, Brison O and Bernheim A: Alternative pathways of MYCN gene copy number increase in primary neuroblastoma tumors. *Cancer Genet Cytogenet* 153: 10-15, 2004.
8. Schwab M, Alitalo K, Klempnauer KH, Varmus HE, Bishop JM, Gilbert F, Brodeur G, Goldstein M and Trent J: Amplified DNA with limited homology to myc cellular oncogene is shared by human neuroblastoma cell lines and a neuroblastoma tumour. *Nature* 305: 245-248, 1983.

9. Edsjö A, Nilsson H, Vandesompele J, Karlsson J, Pattyn F, Culp LA, Speleman F and Pålman S: Neuroblastoma cells with overexpressed MYCN retain their capacity to undergo neuronal differentiation. *Lab Invest* 84: 406-417, 2004.
10. White PS, Thompson PM, Gotoh T, Okawa ER, Igarashi J, Kok M, Winter C, Gregory SG, Hogarty MD, Maris JM and Brodeur GM: Definition and characterization of a region of 1p36.3 consistently deleted in neuroblastoma. *Oncogene* 24: 2684-2694, 2005.
11. Henrich KO, Schwab M and Westermann F: 1p36 tumor suppression-a matter of dosage? *Cancer Res* 72: 6079-6088, 2012.
12. Aygun N: Biological and genetic features of neuroblastoma and their clinical importance. *Curr Pediatr Rev* 14: 73-90, 2018.
13. Raschella G, Negroni A, Skorski T, Pucci S, Nieborowska-Skorska M, Romeo A and Calabretta B: Inhibition of proliferation by *c-myb* antisense RNA and oligodeoxynucleotides in transformed neuroectodermal cell lines. *Cancer Res* 52: 4221-4226, 1992.
14. Thiele CJ, Reynolds CP and Israel MA: Decreased expression of N-myc precedes retinoic acid-induced morphological differentiation of human neuroblastoma. *Nature* 313: 404-406, 1985.
15. Thiele CJ, Cohen PS and Israel MA: Regulation of *c-myb* expression in human neuroblastoma cells during retinoic acid-induced differentiation. *Mol Cell Biol* 8: 1677-1683, 1988.
16. Abemayor E and Sidell N: Human neuroblastoma cell lines as models for the in vitro study of neoplastic and neuronal cell differentiation. *Environ Health Perspect* 80: 3-15, 1989.
17. Aktas S, Altun Z, Erbayraktar Z, Aygun N and Olgun N: Effect of cytotoxic agents and retinoic acid on Myc-N protein expression in neuroblastoma. *Appl Immunohistochem Mol Morphol* 18: 86-89, 2010.
18. Guglielmi L, Cinnella C, Nardella M, Maresca G, Valentini A, Mercanti D, Felsani A and D'Agnano I: MYCN gene expression is required for the onset of the differentiation programme in neuroblastoma cells. *Cell Death Dis* 5: e1081, 2014.
19. Nomura N, Takahashi M, Matsui M, Ishii S, Date T, Sasamoto S and Ishizaki R: Isolation of human cDNA clones of myb-related genes, A-myb and B-myb. *Nucleic Acids Res* 16: 11075-11089, 1988.
20. Davidson CJ, Tirouvanziam R, Herzenberg LA and Lipsick JS: Functional evolution of the vertebrate Myb gene family: B-Myb, but neither A-Myb nor c-Myb, complements *Drosophila* Myb in hemocytes. *Genetics* 169: 215-229, 2005.
21. Beall EL, Manak JR, Zhou S, Bell M, Lipsick JS and Botchan MR: Role for a *Drosophila* Myb-containing protein complex in site-specific DNA replication. *Nature* 420: 833-837, 2002.
22. Lu L, Zhang H and Tower J: Functionally distinct, sequence-specific replicator and origin elements are required for *Drosophila chorion* gene amplification. *Genes Dev* 15: 134-146, 2001.
23. Lewis PW, Beall EL, Fleischer TC, Georgette D, Link AJ and Botchan MR: Identification of a *Drosophila* Myb-E2F2/RBF transcriptional repressor complex. *Genes Dev* 18: 2929-2940, 2004.
24. Koga H, Matsui S, Hirota T, Takebayashi S, Okumura K and Saya H: A human homolog of *Drosophila* lethal(3)malignant brain tumor (l(3)mbt) protein associates with condensed mitotic chromosomes. *Oncogene* 18: 3799-3809, 1999.
25. Gurvich N, Perna F, Farina A, Voza F, Menendez S, Hurwitz J and Nimer SD: L3MBTL1 polycomb protein, a candidate tumor suppressor in del(20q12) myeloid disorders, is essential for genome stability. *Proc Natl Acad Sci USA* 107: 22552-22557, 2010.
26. Fujita M: Cdt1 revisited: Complex and tight regulation during the cell cycle and consequences of deregulation in mammalian cells. *Cell Div* 1: 22, 2006.
27. Karakaidos P, Taraviras S, Vassiliou LV, Zacharatos P, Kastrinakis NG, Kougiou D, Kouloukoussa M, Nishitani H, Papavassiliou AG, Lygerou Z and Gorgoulis VG: Overexpression of the replication licensing regulators hCdt1 and hCdc6 characterizes a subset of non-small-cell lung carcinomas: Synergistic effect with mutant p53 on tumor growth and chromosomal instability-evidence of E2F-1 transcriptional control over hCdt1. *Am J Pathol* 165: 1351-1365, 2004.
28. Xouri G, Lygerou Z, Nishitani H, Pachnis V, Nurse P and Taraviras S: Cdt1 and geminin are down-regulated upon cell cycle exit and are over-expressed in cancer-derived cell lines. *Eur J Biochem* 271: 3368-3378, 2004.
29. Wohlschlegel JA, Kutok JL, Weng AP and Dutta A: Expression of geminin as a marker of cell proliferation in normal tissues and malignancies. *Am J Pathol* 161: 267-273, 2002.
30. Chen L, Iraci N, Gherardi S, Gamble LD, Wood KM, Perini G, Lunec J and Tweddle DA: p53 is a direct transcriptional target of MYCN in neuroblastoma. *Cancer Res* 70: 1377-1388, 2010.
31. Eckerle I, Muth D, Batzler J, Henrich KO, Lutz W, Fischer M, Witt O, Schwab M and Westermann F: Regulation of BIRC5 and its isoform BIRC5-2B in neuroblastoma. *Cancer Lett* 285: 99-107, 2009.
32. Petroni M, Veschi V, Prodosmo A, Rinaldo C, Massimi I, Carbonari M, Dominici C, McDowell HP, Rinaldi C, Screpanti I, et al: MYCN sensitizes human neuroblastoma to apoptosis by HIPK2 activation through a DNA damage response. *Mol Cancer Res* 9: 67-77, 2011.
33. Liu DX, Biswas SC and Greene LA: B-Myb and C-Myb play required roles in neuronal apoptosis evoked by nerve growth factor deprivation and DNA damage. *J Neurosci* 24: 8720-8725, 2004.
34. Aygun N and Altungoz O: Novel structural abnormalities involving chromosomes 1, 17 and 2 identified by fluorescence in situ hybridization (FISH) and/or cytogenetic karyotyping in Kelly and SH-SY5Y human neuroblastoma cell lines, respectively. *J Can Res Updates* 6: 46-55, 2017.
35. Protocol for DNA extraction. DNA preparation from adherent cells. Section of Cancer Genomics, Genetics Branch, NCI National Institutes of Health 2 pages, 2006. Available from: [https://ccr.cancer.gov/sites/default/files/dna\\_prep\\_from\\_adherent\\_cells.pdf](https://ccr.cancer.gov/sites/default/files/dna_prep_from_adherent_cells.pdf).
36. Pfaffl MW: A new mathematical model for relative quantification in real-time RT-PCR. *Nucleic Acids Res* 29: e45, 2001.
37. Babicki S, Arndt D, Marcu A, Liang Y, Grant JR, Maciejewski A and Wishart DS: Heatmapper: Web-enabled heat mapping for all. *Nucleic Acids Res* 44: W147-W153, 2016.
38. Rasmussen R: Quantification on the LightCycler. In: Meuer S, Wittwer C, Nakagawara K, (eds). *Rapid cycle real-time PCR, methods and applications*. Heidelberg, Springer Press, pp21-34, 2001.
39. Aksakoglu G: Korelasyon ve regresyon (Correlation and regression): Sağlıkta araştırma teknikleri ve analiz yöntemleri (Research techniques and analysis methods in health). 1st ed. Dokuz Eylül University Press, Izmir, pp305-346, 2001 (In Turkish).
40. Hiller S, Breit S, Wang ZQ, Wagner EF and Schwab M: Localization of regulatory elements controlling human MYCN expression. *Oncogene* 6: 969-977, 1991.
41. Tower J: Developmental gene amplification and origin regulation. *Annu Rev Genet* 38: 273-304, 2004.
42. Wright JA, Smith HS, Watt FM, Hancock MC, Hudson DL and Stark GR: DNA amplification is rare in normal human cells. *Proc Natl Acad Sci USA* 87: 1791-1795, 1990.
43. Himoudi N, Yan M, Papanastasiou A and Anderson J: MYCN as a target for cancer immunotherapy. *Cancer Immunol Immunother* 57: 693-700, 2008.
44. Orr-Weaver TL and Spradling AC: *Drosophila* chorion gene amplification requires an upstream region regulating sl8 transcription. *Mol Cell Biol* 6: 4624-4633, 1986.
45. Imamura Y, Iguchi-Aruga SM and Ariga H: The upstream region of the mouse N-myc gene: Identification of an enhancer element that functions preferentially in neuroblastoma IMR32 cells. *Biochim Biophys Acta* 1132: 177-187, 1992.
46. Chen H, Li H, Liu F, Zheng X, Wang S, Bo X and Shu W: An integrative analysis of TFBS-clustered regions reveals new transcriptional regulation models on the accessible chromatin landscape. *Sci Rep* 5: 8465, 2015.
47. Zhu W, Giangrande PH and Nevins JR: E2Fs link the control of G1/S and G2/M transcription. *EMBO J* 23: 4615-4626, 2004.
48. Nakata Y, Shetzline S, Sakashita C, Kalota A, Rallapalli R, Rudnick SI, Zhang Y, Emerson SG and Gewirtz AM: c-Myb contributes to G2/M cell cycle transition in human hematopoietic cells by direct regulation of cyclin B1 expression. *Mol Cell Biol* 27: 2048-2058, 2007.
49. Tarasov KV, Tarasova YS, Tam WL, Riordon DR, Elliott ST, Kania G, Li J, Yamanaka S, Crider DG, Testa G, et al: B-MYB is essential for normal cell cycle progression and chromosomal stability of embryonic stem cells. *PLoS One* 3: e2478, 2008.
50. Kreis NN, Sanhaji M, Rieger MA, Louwen F and Yuan J: p21Waf1/Cip1 deficiency causes multiple mitotic defects in tumor cells. *Oncogene* 33: 5716-5728, 2014.
51. Strieder V and Lutz W: E2F proteins regulate MYCN expression in neuroblastomas. *J Biol Chem* 278: 2983-2989, 2003.

52. Yoshida K and Inoue I: Regulation of Geminin and Cdt1 expression by E2F transcription factors. *Oncogene* 23: 3802-3812, 2004.
53. Radhakrishnan SK, Feliciano CS, Najmabadi F, Haegbarth A, Kandel ES, Tyner AL and Gartel AL: Constitutive expression of E2F-1 leads to p21-dependent cell cycle arrest in S phase of the cell cycle. *Oncogene* 23: 4173-4176, 2004.
54. Sala A, Casella I, Bellon T, Calabretta B, Watson RJ and Peschle C: B-myb promotes S phase and is a downstream target of the negative regulator p107 in human cells. *J Biol Chem* 271: 9363-9367, 1996.
55. Markey M, Siddiqui H and Knudsen ES: Geminin is targeted for repression by the retinoblastoma tumor suppressor pathway through intragenic E2F sites. *J Biol Chem* 279: 29255-29262, 2004.
56. Sala A, Nicolaides NC, Engelhard A, Bellon T, Lawe DC, Arnold A, Graña X, Graña X, Giordano A and Calabretta B: Correlation between E2F-1 requirement in the S phase and E2F-1 transactivation of cell cycle-related genes in human cells. *Cancer Res* 54: 1402-1406, 1994.
57. Brodeur GM: Neuroblastoma: Biological insights into a clinical enigma. *Nat Rev Cancer* 3: 203-216, 2003.
58. Stiewe T and Pützner BM: Role of the p53-homologue p73 in E2F1-induced apoptosis. *Nat Genet* 26: 464-469, 2000.
59. Goldschneider D, Blanc E, Raguénez G, Barrois M, Legrand A, Le Roux G, Haddada H, Bénard J and Douc-Rasy S: Differential response of p53 target genes to p73 overexpression in SH-SY5Y neuroblastoma cell line. *J Cell Sci* 117: 293-301, 2004.
60. Fontana L, Fiori ME, Albini S, Cifaldi L, Giovinazzi S, Forloni M, Boldrini R, Donfrancesco A, Federici V, Giacomini P, *et al*: Antagomir-17-5p abolishes the growth of therapy-resistant neuroblastoma through p21 and BIM. *PLoS One* 3: e2236, 2008.
61. Tang XX, Zhao H, Kung B, Kim DY, Hicks SL, Cohn SL, Cheung NK, Seeger RC, Evans AE and Ikegaki N: The MYCN enigma: Significance of MYCN expression in neuroblastoma. *Cancer Res* 66: 2826-2833, 2006.
62. Jost CA, Marin MC and Kaelin WG Jr: p73 is a human p53-related protein that can induce apoptosis. *Nature* 389: 191-194, 1997.
63. Kaghad M, Bonnet H, Yang A, Creancier L, Biscan JC, Valent A, Minty A, Chalon P, Lelias JM, Dumont X, *et al*: Monoallelically expressed gene related to p53 at 1p36, a region frequently deleted in neuroblastoma and other human cancers. *Cell* 90: 809-819, 1997.
64. Lau LM, Wolter JK, Lau JT, Cheng LS, Smith KM, Hansford LM, Zhang L, Baruchel S, Robinson F and Irwin MS: Cyclooxygenase inhibitors differentially modulate p73 isoforms in neuroblastoma. *Oncogene* 28: 2024-2033, 2009.
65. Fukasawa K, Wiener F, Vande Woude GF and Mai S: Genomic instability and apoptosis are frequent in p53 deficient young mice. *Oncogene* 15: 1295-1302, 1997.
66. Prochazka P, Hrabeta J, Vicha A, Cipro S, Stejskalova E, Musil Z, Vodicka P and Eckschlager T: Changes in MYCN expression in human neuroblastoma cell lines following cisplatin treatment may not be related to MYCN copy numbers. *Oncol Rep* 29: 2415-2421, 2013.
67. Henrichsen CN, Chaignat E and Reymond A: Copy number variants, diseases and gene expression. *Hum Mol Genet* 18: R1-R8, 2009.
68. Sexton T, Umlauf D, Kurukuti S and Fraser P: The role of transcription factories in large-scale structure and dynamics of interphase chromatin. *Semin Cell Dev Biol* 18: 691-697, 2007.
69. Pihan GA, Purohit A, Wallace J, Knecht H, Woda B, Quesenberry P and Doherty SJ: Centrosome defects and genetic instability in malignant tumors. *Cancer Res* 58: 3974-3985, 1998.
70. Adon AM, Zeng X, Harrison MK, Sannem S, Kiyokawa H, Kaldis P and Saavedra HI: Cdk2 and Cdk4 regulate the centrosome cycle and are critical mediators of centrosome amplification in p53-null cells. *Mol Cell Biol* 30: 694-710, 2010.
71. Sugihara E, Kanai M, Matsui A, Onodera M, Schwab M and Miwa M: Enhanced expression of MYCN leads to centrosome hyperamplification after DNA damage in neuroblastoma cells. *Oncogene* 23: 1005-1009, 2004.
72. Mantel C, Braun SE, Reid S, Henegariu O, Liu L, Hangoc G and Broxmeyer HE: p21(cip-1/waf-1) deficiency causes deformed nuclear architecture, centriole overduplication, polyploidy, and relaxed microtubule damage checkpoints in human hematopoietic cells. *Blood* 93: 1390-1398, 1999.
73. Stewart ZA, Leach SD and Pietsenpol JA: p21(Waf1/Cip1) inhibition of cyclin E/Cdk2 activity prevents endoreduplication after mitotic spindle disruption. *Mol Cell Biol* 19: 205-215, 1999.
74. Chen J, Willingham T, Shuford M, Bruce D, Rushing E, Smith Y and Nisen PD: Effects of ectopic overexpression of p21(WAF1/CIP1) on aneuploidy and the malignant phenotype of human brain tumor cells. *Oncogene* 13: 1395-1403, 1996.
75. Quinn LM, Herr A, McGarry TJ and Richardson H: The *Drosophila* geminin homolog: Roles for Geminin in limiting DNA replication, in anaphase and in neurogenesis. *Genes Dev* 15: 2741-2754, 2001.
76. Clijsters L, Ogink J and Wolthuis R: The spindle checkpoint, APC/C(Cdc20), and APC/C(Cdh1) play distinct roles in connecting mitosis to S phase. *J Cell Biol* 201: 1013-1026, 2013.
77. Biedler JL and Spengler BA: A novel chromosome abnormality in human neuroblastoma and antifolate-resistant Chinese hamster cell lines in culture. *J Natl Cancer Inst* 57: 683-695, 1976.
78. Amler LC and Schwab M: Amplified N-myc in human neuroblastoma cells is often arranged as clustered tandem repeats of differently recombined DNA. *Mol Cell Biol* 9: 4903-4913, 1989.
79. Lo AW, Sabatier L, Fouladi B, Pottier G, Ricoul M and Murnane JP: DNA amplification by breakage/fusion/bridge cycles initiated by spontaneous telomere loss in a human cancer cell line. *Neoplasia* 4: 531-538, 2002.
80. Schwab M: Human neuroblastoma: From basic science to clinical debut of cellular oncogenes. *Naturwissenschaften* 86: 71-78, 1999.
81. Watanabe T, Tanabe H and Horiuchi T: Gene amplification system based on double rolling-circle replication as a model for oncogene-type amplification. *Nucleic Acids Res* 39: e106, 2011.
82. Blumrich A, Zaparka M, Brueckner LM, Zheglo D, Schwab M and Savelyeva L: The FRA2C common fragile site maps to the borders of MYCN amplicons in neuroblastoma and is associated with gross chromosomal rearrangements in different cancers. *Hum Mol Genet* 20: 1488-1501, 2011.
83. Slack A, Thornton PC, Magner DB, Rosenberg SM and Hastings PJ: On the mechanism of gene amplification induced under stress in *Escherichia coli*. *PLoS Genet* 2: e48, 2006.
84. Aygun N: Acquired chromosomal abnormalities and their potential formation mechanisms in solid tumours. In: *Chromosomal abnormalities-a hallmark manifestation of genomic instability*. Larramendy M, (ed.) InTech, pp27-70, 2017. Available from: <https://www.intechopen.com/books/chromosomal-abnormalities-a-hallmark-manifestation-of-genomic-instability/acquired-chromosomal-abnormalities-and-their-potential-formation-mechanisms-in-solid-tumours>.
85. Forbes SA, Beare D, Boutselakis H, Bamford S, Bindal N, Tate J, Cole CG, Ward S, Dawson E, Ponting L, *et al*: COSMIC: Somatic cancer genetics at high-resolution. *Nucleic Acids Res* 45: D777-D783, 2017.
86. Aygun N: Correlations between long inverted repeat (LIR) features, deletion size and distance from breakpoint in human gross gene deletions. *Sci Rep* 5: 8300, 2015.
87. Lai PJ, Lim CT, Le HP, Katayama T, Leach DR, Furukohri A and Maki H: Long inverted repeat transiently stalls DNA replication by forming hairpin structures on both leading and lagging strands. *Genes Cells* 21: 136-145, 2016.
88. Voineagu I, Narayanan V, Lobachev KS and Mirkin SM: Replication stalling at unstable inverted repeats: Interplay between DNA hairpins and fork stabilizing proteins. *Proc Natl Acad Sci USA* 105: 9936-9941, 2008.
89. Conrad DF, Bird C, Blackburne B, Lindsay S, Mamanova L, Lee C, Turner DJ and Hurler ME: Mutation spectrum revealed by breakpoint sequencing of human germline CNVs. *Nat Genet* 42: 385-391, 2010.
90. Hastings PJ, Ira G and Lupski JR: A microhomology-mediated break-induced replication model for the origin of human copy number variation. *PLoS Genet* 5: e1000327, 2009.



This work is licensed under a Creative Commons Attribution-NonCommercial-NoDerivatives 4.0 International (CC BY-NC-ND 4.0) License.